

Review

Trends in Molecularly Imprinted Polymers (MIPs)-Based Plasmonic Sensors

Giancarla Alberti ^{1,*} , Camilla Zanoni ¹, Stefano Spina ¹, Lisa Rita Magnaghi ^{1,2}  and Raffaella Biesuz ^{1,2}¹ Department of Chemistry, University of Pavia, Via Taramelli 12, 27100 Pavia, Italy² Unità di Ricerca di Pavia, Consorzio Interuniversitario Nazionale per la Scienza e Tecnologia dei Materiali, INSTM, Via G. Giusti 9, 50121 Firenze, Italy

* Correspondence: galberti@unipv.it

Abstract: In recent years, plasmonic sensors have been used in various fields ranging from environmental monitoring, pharmaceutical analysis, medical diagnosis, and food quality assessment to forensics. A significant amount of information on plasmonic sensors and their applications already exists and there is a continuing development of reliable, selective, sensitive, and low-cost sensors. Combining molecularly imprinting technology with plasmonic sensors is an increasingly timely and important challenge to obtain portable, easy-to-use, particularly selective devices helpful in detecting analytes at the trace level. This review proposes an overview of the applications of molecularly imprinted plasmonic chemosensors and biosensors, critically discussing the performances, pros, and cons of the more recently developed devices.

Keywords: plasmonic chemosensors; plasmonic biosensors; molecularly imprinted polymer sensors; chemical analyses; biochemical analyses; nanoparticles; MIP-based sensors; low-cost devices; high selectivity-sensors



Citation: Alberti, G.; Zanoni, C.; Spina, S.; Magnaghi, L.R.; Biesuz, R. Trends in Molecularly Imprinted Polymers (MIPs)-Based Plasmonic Sensors. *Chemosensors* **2023**, *11*, 144. <https://doi.org/10.3390/chemosensors11020144>

Academic Editor: Pi-Guey Su

Received: 23 January 2023

Revised: 10 February 2023

Accepted: 13 February 2023

Published: 15 February 2023



Copyright: © 2023 by the authors. Licensee MDPI, Basel, Switzerland. This article is an open access article distributed under the terms and conditions of the Creative Commons Attribution (CC BY) license (<https://creativecommons.org/licenses/by/4.0/>).

1. Introduction

The application of Molecularly Imprinted Polymers (MIPs) as sensing recognition elements in chemo-/biosensors has been continuously developing since the 1990s [1–7]. MIPs are appealing for recognition properties like those of biological receptors but with higher stability and for their availability for several target analytes. These pros have confirmed MIPs' application in different fields, like solid-phase extraction (SPE), immune tests, drug delivery, and sensing [7–9].

Molecular imprinting is a template-guided synthesis resulting in the formation of selective cavities in a polymeric network [10]. The removal of the template from the polymer left cavities that are complementary in shape and dimension to the same molecule template (see Figure 1, [11]).

Research on MIPs has enticed scientific interest due to promising characteristics like stability, robustness, selectivity, and high affinity towards the target analyte [12–17]. The groundbreaking approach of MIP-based sensors for environmental and biomedical analysis can be explained by their ability to selectively detect target molecules present in complex matrices at trace levels, frequently without the need for sample pretreatment, which could open the possibility of in-situ monitoring and clinical tests at the point-of-care. Unfortunately, the research and development of MIP-based sensor technology are still at the academic level [18].

Most MIP-based sensors exploit optical or electrochemical responses. Among the optical sensors, Surface Plasmon Resonance (SPR) and Localized Surface Plasmon Resonance (LSPR) are, to date, the most promising MIP-faced devices.

SPR and LSPR sensors have appealing characteristics like suitability for automation, the possibility for label-free analysis, and easy surface modification to be effectively functionalized with MIPs [19].

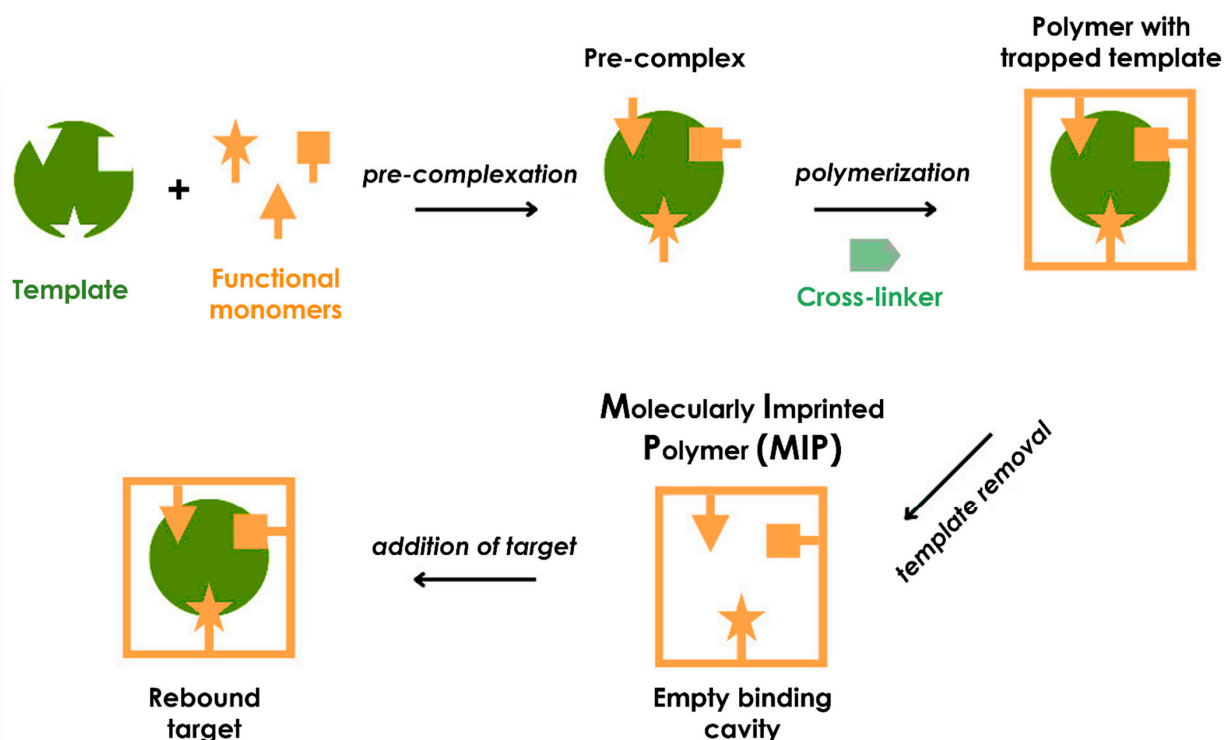


Figure 1. Molecularly imprinted polymers (MIPs) synthesis. (Reproduced with permission from [11], open access Creative Common CC licensed 4.0, MDPI).

Surface plasmons are free electrons coherent oscillations at a metal/dielectric interface that are classified into two groups: propagating surface plasmons and localized surface plasmons [20].

SPR sensors use the evanescent field of surface plasmons propagating through a metallic surface to detect variations of the sample's dielectric constant around 100 nm of the plasmonic material. The interaction of the evanescent field with the analyte produces a shift in transmitted excitation light wavelength (or angle) or a change in light intensity proportional to the changes in the sample's refractive index [21–24]. This change allows detection of the target analyte.

When the surface plasmon is constrained to a nanoparticle of a size like the light's wavelength, the particle's free electrons contribute to the coherent oscillation. This phenomenon is called Localized Surface Plasmon Resonance (LSPR). LSPR shows two significant effects: the electric field close to the nanoparticle's surface is considerably enhanced, and the nanoparticle's optical transmission spectrum shows a maximum at the plasmon resonant frequency in the region of the UV-vis that depends on the refractive index of the surrounding medium [25]. The plasmon resonance spectral shift determined by a change in the dielectric properties of the environment surrounding the metal nanoparticles is the sensing principle for LSPR sensors [26]. A scheme of SPR and LSPR mechanisms is shown in Figure 2 [27].

In the last thirty years, there has been a huge increase in fiber-optic-based sensors for applications in several fields, like the environment, agriculture, food industries, energy, pharmaceuticals, and medicine, thanks to their peculiar features that allow remote or online monitoring and the possibility of obtaining miniaturized devices suitable for point-of-care measurements [28]. In optical fiber sensors, the fiber can be simply used as a waveguide to carry light from a source to a sensing component; this is the case for the so-called extrinsic sensors. Otherwise, intrinsic platforms are obtained when the optical fiber itself is used as a sensing waveguide. In this scenario, SPR/LSPR implementation on optical fibers was exploited, aiming to obtain very sensitive and small-size sensors [29–31].

Additionally, highly selective platforms can be produced by modifying the SPR/LSPR surfaces with receptors, such as MIPs.

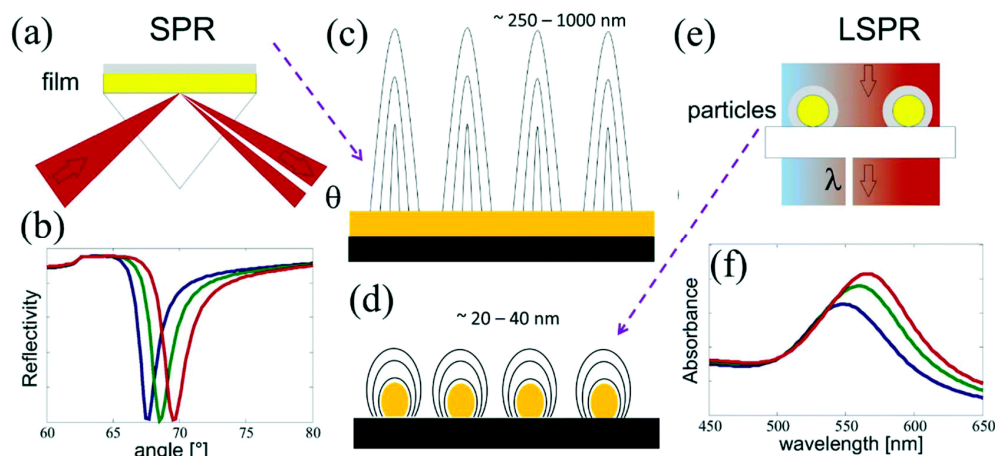


Figure 2. Scheme of SPR (a–c) and LSPR (d–f) mechanisms. λ is the wavelength [nm] and θ the angle of reflection [°]. (Reproduced with permission from [27], open access Creative Common CC licensed 3.0, Royal Chemical Society—RSC).

This paper presents an overview of molecularly imprinted plasmonic chemosensors and biosensors. Their realization and applications will be critically discussed. Compared to other recent reviews on the same topic, but more sectoral and specific (see, for example, Gupta et al. [28], Cennamo et al. [31] and Yang et al. [32] for MIPs-based optical fiber sensors or Chiappini et al. [33] for biosensors or Fang et al. [34] for MIPs-modified optical sensors for pesticides), the present review provides a broader overview of the state of the art SPR and LSPR sensors interfaced with molecularly imprinted polymers for applications in various fields, including environmental, agricultural, and clinical-biomedical.

2. MIP-Based Plasmonic Chemosensors and Biosensors

The following paragraphs describe the latest advances in SPR and LSPR sensors functionalized with molecularly imprinted polymers (MIPs). Devices based on MIP film covering the plasmonic surfaces, nanoMIP-based chips, MIP-coated nanoparticles-based sensors, and MIP films-based SPR imaging chips will be presented together with their analytical applications.

2.1. MIP Film-Based SPR Sensors

The first MIP-based SPR sensor was proposed by Lai et al. for caffeine, theophylline, and xanthine detection [35]. After this pioneering work, the employment of MIP as a recognition element in SPR sensors become an appealing strategy for developing selective and sensitive sensors for various target molecules of environmental, biological, clinical, and industrial interest [24].

In MIP film-based devices, a surface imprinting with control of the polymer layer thickness must be performed to ensure the measurements' good reproducibility [36].

Drop-coating and spin-coating of the prepolymeric MIP's mixture are the common techniques with the spin-coating approach the best one for nanosized control of the MIP layer thickness [36,37].

The Zeni and Cennamo group proposed several MIP-functionalized SPR sensors based on D-shaped plastic optical fibers (POFs). These platforms were realized by eliminating both the cladding and the partial core of the optical fiber, spin coating a photoresist buffer layer (Microposit S1813) on the exposed core, and sputtering a gold film over the buffer [38]. Finally, the MIP prepolymeric mixture was drop-coated or spin-coated on the gold sensing surface and left to polymerize overnight thermally. Figure 3 reports a scheme of this kind of platform [39].

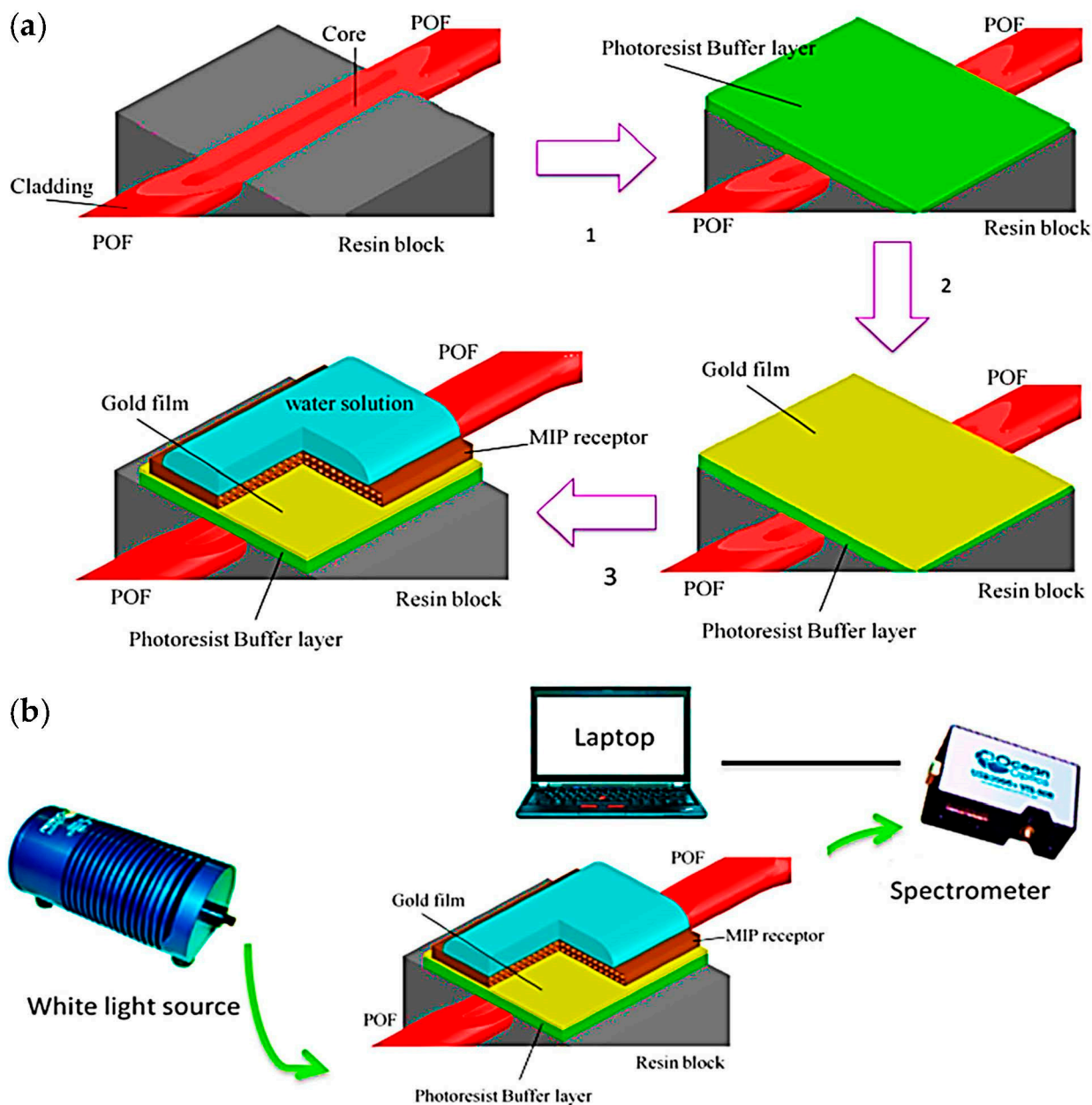


Figure 3. (a) Steps to realize a MIP-based SPR sensor in a D-shaped POF; (b) outline of the experimental setup. (Reproduced with permission from [39], open access Creative Common CC licensed 4.0, MDPI).

In SPR-POF platforms, an increase in the refractive index at the gold/dielectric interface, according to the SPR theory, corresponds to a shift in the resonance wavelength [38]. When a MIP layer covers the gold film, the interaction of the target analyte with the MIP cavities usually produces an increase in the resonance wavelength due to the refractive index variation at the interface MIP layer/gold film [39].

An example of these sensors is a MIP on a plasmonic POF for detecting perfluorinated compounds [39]. The sensor was very selective for perfluorooctanoate, perfluorooctanesulfonate, and perfluorinated alkylated substances in the C₄–C₁₁ range, with a LOD of about 0.1 µg/L.

A similar experimental setup was applied, with satisfying performances, for the detection of 2-furaldehyde in transformer oil and wine samples [40,41], 2,4,6-trinitrotoluene (TNT) in water [42], L-nicotine in aqueous solution [43], for the simultaneous detection

of dibenzyl disulfide and 2-furaldehyde in electrical transformers insulating oil [44], and recently for SARS-CoV-2 in swab and physiological solutions [45].

Always using the spin-coating of the prepolymeric mixture of MIPs, Dibekkaya et al. [46] proposed an SPR sensor to detect cyclic citrullinated peptide antibodies (anti-CCP). A pre-complex was prepared by adding acrylamide monomer (Aam) to anti-CCP. Then, the SPR sensor was obtained by reacting the pre-complex with the cross-linker and the initiator/activator pair, forming a nanofilm monolayer.

Another interesting work is that proposed by Ayankojo et al. [47]; in this case, a hybrid inorganic-organic MIP film selective for amoxicillin was prepared and integrated with an SPR sensor. The film was obtained by a sol-gel procedure and employing tetraethoxysilane as an inorganic precursor, methacrylamide as the organic functional monomer, and vinyltrimethoxysilane as a coupling agent. Prepared in this way, the MIP-based SPR platform permitted the highly sensitive and selective amoxicillin determination showing a detection limit down to 70 pM and the possibility to discriminate the target analyte among structurally similar molecules both in synthetic buffer solutions and tap water samples with good reproducibility of the measurements.

The MIP layer's thickness can also be monitored by constraining the pre-polymerization mixture between two flat surfaces and applying continuous pressure during the polymerization step. This method is called microcontact imprinting. One of the surfaces functions as the substrate for the resulting MIP, while the other is functionalized with the template molecule. This method permits a surface imprint of the polymer [48], and it is particularly of interest for imprinting high molecular weight molecules, such as microorganisms or biomolecules [48–50]. For example, a microcontact-imprinted SPR sensor for the pathogenic bacteria *S. paratyphi* was developed by Perçin et al. [49]. To begin, preparation and modification of glass slides were undertaken. Amino groups were introduced with 3% 3-amino-propyltriethoxysilane (APTES). Then, the amino groups were derivatized by glutaraldehyde, and *S. paratyphi* cells were added to the glass surface. In parallel, the gold surface of SPR chips was modified with allyl mercaptan ($\text{CH}_2\text{CHCH}_2\text{SH}$). The microcontact imprinting of *S. paratyphi* onto the SPR chips was then realized. The aminoacid-modified acrylate N-methacryloyl L-histidine methyl ester (MAH) was mixed with a Cu(II) salt to form a Cu(II)-MAH complex. Then, 2-hydroxyethyl methacrylate (HEMA), ethylene glycol dimethacrylate (EGDMA), and azobis-isobutyronitrile (AIBN) were added and the obtained solution was placed on the SPR chip. The glass slide with immobilized *S. paratyphi* was placed in contact with the monomer solution on the SPR chip, and UV-vis polymerization was performed. Figure 4 shows a scheme of this microcontact imprinting process [49]. With the proposed SPR sensor, the recognition of *S. paratyphi* was achieved with a detection limit (LOD) of 1.4×10^6 CFU/mL. The sensor's selectivity was verified using *Escherichia coli*, *Staphylococcus aureus*, and *Bacillus subtilis* as competing bacterial strains. Additionally, experiments with the target microorganisms in apple juice were undertaken. The strong results highlighted the sensor's potential for *S. paratyphi* detection in water and food samples.

A similar approach was employed by Bergdahl et al. [50] for in vivo detection of a bacterial factor (RoxP) secreted by the skin. Figure 5 depicts a scheme of the sensor preparation by microcontact imprinting.

The MIP composition was optimized, characterizing five different polymeric mixtures. The best performances were achieved with 2-Hydroxyethyl methacrylate as monomer and poly(ethylene glycol) dimethacrylate as a cross-linker, obtaining a MIP-chip with a detection limit of about 0.2 nM. This study offers an effective sensor for detecting and quantifying RoxP as a marker for oxidative stress on the skin.

A surface-grafted MIP film obtained by radical photopolymerization combined with microcontact imprinting aimed at developing a BSA (Bovine Serum Albumin) SPR sensor was proposed by Kidakova et al. [51]. The reversible addition-fragmentation chain transfer (RAFT) controlled-living radical polymerization method was applied since it allowed better control of the thickness and composition of molecularly imprinted polymer film, as

previously verified [52–54]. With the perspective of preparing a MIP film of protein with homogeneous cavities confined on the surface, microcontact imprinting was the elected strategy [55–57]. By this synthetic approach, a thin film of polymethacrylate molecularly imprinted with BSA was placed directly in contact with the SPR chip surface. The sensor response was pseudo-linear in a restricted range of BSA concentration (from 2.5 nM to 25 nM) with a detection limit of about 6 nM. In any case, the simple synthetic procedure is promising for developing MIP-based sensors for other proteins of clinical interest.

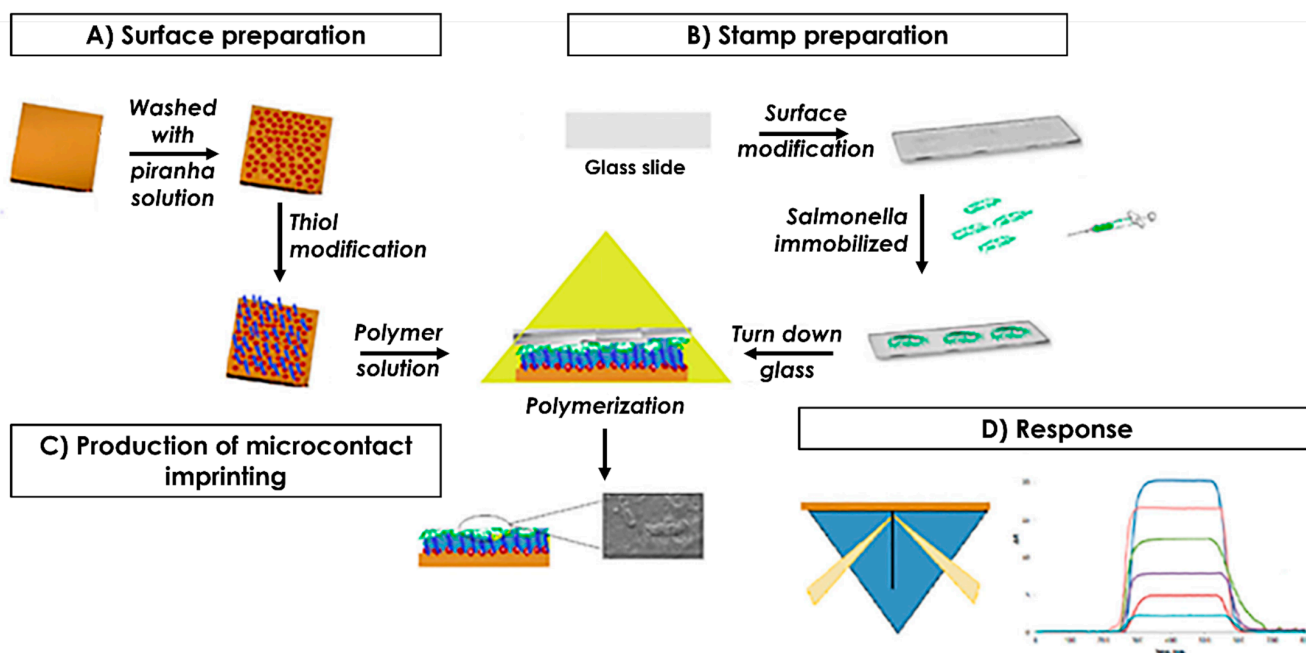


Figure 4. Scheme of the microcontact imprinting of *S. paratyphi* onto SPR chips. (A) preparation and modification of the SPR chip surface; (B) imprinting of *S. paratyphi* on a glass slide; (C) realization of the microcontact imprinting; (D) response of the SPR sensor. (Reproduced with permission from [49], open access Creative Common CC licensed 4.0, MDPI).

As described below, in-situ polymerization of molecularly-imprinted thin films was generally obtained by different approaches like drop-coating, spin-coating, or layer-by-layer deposition and recently mixed methods based on nanotechnology. Few papers and reviews have addressed the electrochemical methodology. Molecular imprinting performed by this technique is appealing for developing sensors for different applications and based on different transduction, including SPR devices. Compared to the previously described methods, the MIP electrosynthesis can often be performed in aqueous solutions and allows film thickness control via electrochemical parameters [58]. Generally, the MIP electropolymerization on SPR sensors requires a three-electrode cell: the working electrode is the gold chip surface, the reference is a classical Ag/AgCl electrode, and the counter electrode is a platinum wire or graphite rod.

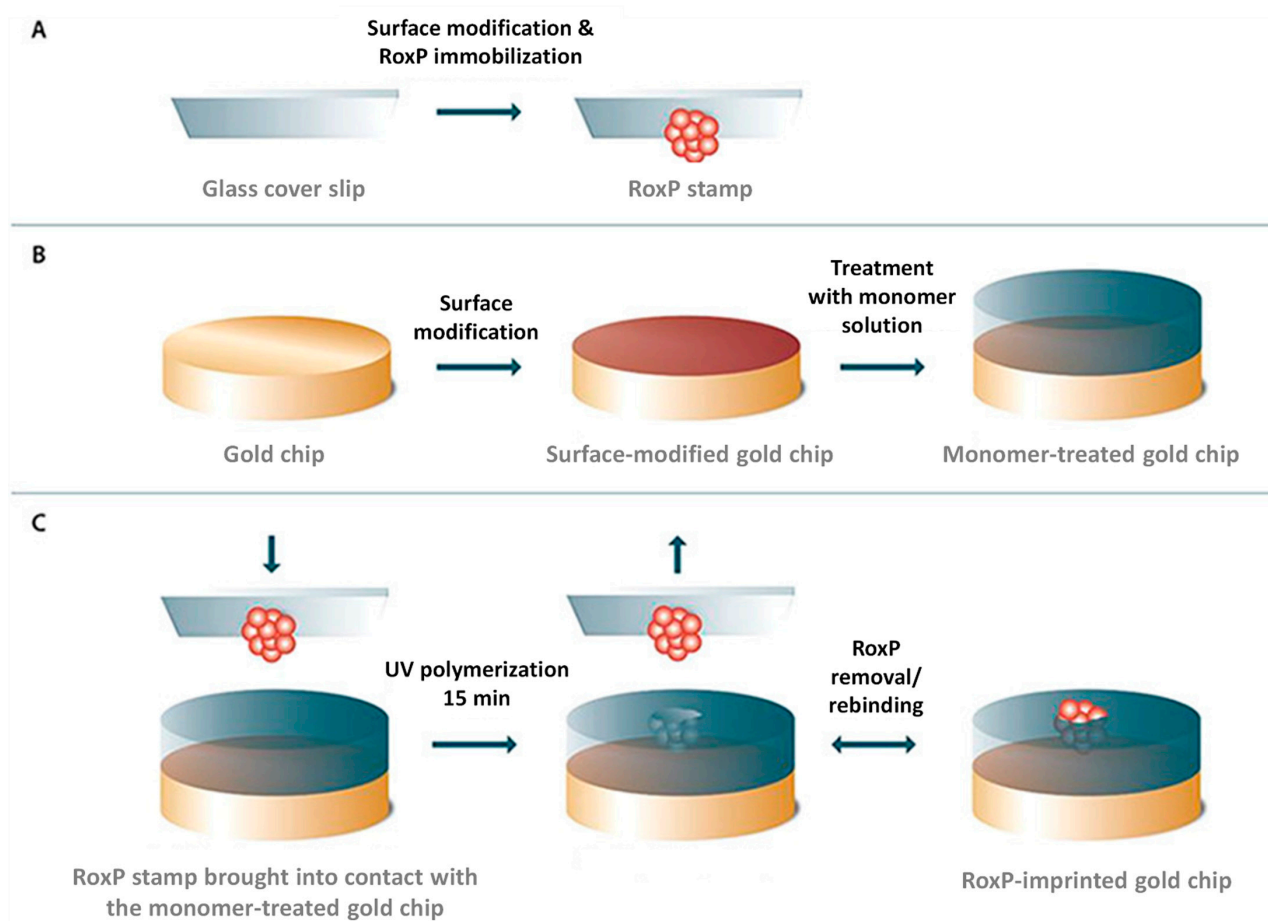


Figure 5. MIP-based SPR sensor for the bacterial factor RoxP: scheme of the MIP layer preparation by microcontact imprinting. (A) Glass cover slip surface modification and RoxP immobilization; (B) gold chip surface modification with the monomer; (C) microcontact of the RoxP stamp with the monomer-treated gold chip and UV imprinting (Reproduced with permission from [50], Copyright © 2019, American Chemical Society).

Adopting this approach, Choi et al. [59] proposed a MIP-based SPR sensor for the mycotoxin zearalenone. The MIP film was obtained by electropolymerization of pyrrole onto the gold surface of the SPR chip in the presence of zearalenone molecule as the template. The linear response was obtained in the range of 0.3–3000 ng/mL. The detection limit and the recovery for corn samples spiked with 30 ng/g of analyte were 0.3 ng/g and 89%, respectively, similar to those achieved by classical enzyme-linked immunosorbent assay (ELISA). The selectivity was also proved by testing structurally related analogs of zearalenone, highlighting the strong affinity of the MIP for the studied mycotoxin.

Functionalized terthiophenes were also exploited for MIP electrosynthesis. Permites et al. proposed the modification of SPR chips by electropolymerized MIPs (e-MIPs) starting from carboxyl functionalized-terthiophene monomers. The sensors were developed for theophylline [60,61], paracetamol, and naproxen [61]. Analogous monomers were employed by Hubilla et al. [62] to prepare an e-MIP-based SPR sensor for histamine detection. The fabricated sensor showed a good linear range from 15 to 500 µg/mL, with a detection limit of 2.0 µg/mL. The high selectivity for histamine was verified by testing histamine analogs such as L-histidine, putrescine, and cadaverine.

An e-MIP prepared in situ by electropolymerization of 3-aminophenylboronic acid on the gold surface on an SPR chip was proposed to detect Staphylococcal Enterotoxin B [63]. The sensors showed very high sensitivity: a linear response from 3.2 fM to 25.6 fM and a detection limit of 0.05 fM were obtained. Interference studies with the homologs of

Staphylococcal Enterotoxin B, such as Staphylococcal Enterotoxin A and C, demonstrated the high affinity of the MIP's cavities for the target analyte.

The same group [64] proposed another interesting study for the detection of T-2 toxin, a bio-toxin potentially used as a biological weapon for terrorist purposes. In this case, a π -conjugated MIP with nanopatterns was prepared on the gold surface of the SPR chip by in situ electropolymerization of 3-aminophenylboronic acid as functional monomers. 3-aminophenylboronic acid was selected since the boronic acid moiety permits reversible electrostatic and covalent interactions with the template molecules as a function of the pH and solvent polarity. The very low detection limit obtained (0.1 fM) makes the device promising since the sensor can detect T-2 toxin below the concentrations recommended by the American subcommittee.

Bartold K. et al. proposed e-MIP-based SPR chips to determine genetically relevant oligonucleotides [65,66]. 2-(cytosin-1-yl)ethyl 4-bis(2,2'-bithien-5-yl)methylbenzoate and 4-bis(2,2'-bithien-5-yl)methylphenyl-2-guanine ethyl were employed as functional monomers, and a peptide nucleic acid (PNA) as the template due to the sequence selectivity and affinity to complementary RNA and DNA single strands. In particular, the developed chemosensors aimed to identify genetically relevant GC-rich (guanidine = G and cytosine = C) oligonucleotides (cancer biomarkers present in the bloodstream as cell-free DNA), so C-term-GCGGCGGC-N-term single-stranded PNA was synthesized.

A scheme of the e-MIP synthesis and the binding of the target analyte is shown in Figure 6.

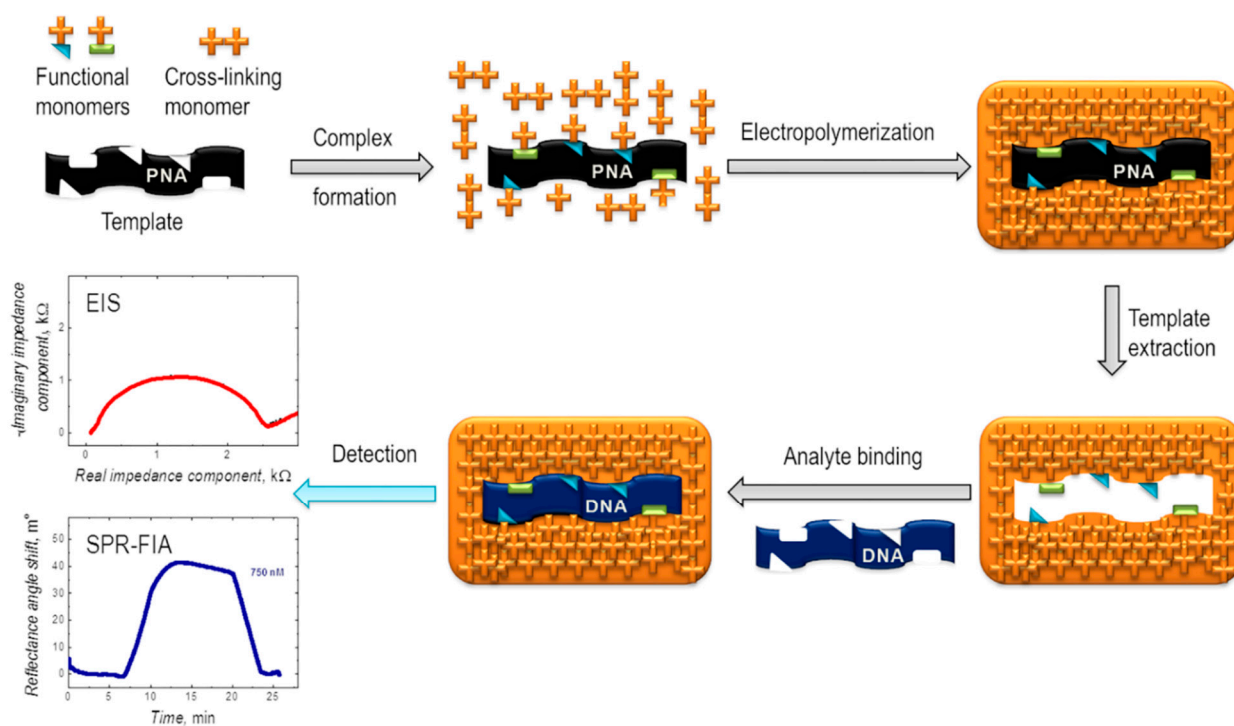


Figure 6. Scheme of the e-MIP using C-Term-GCGGCGGC-N-Term Single-Stranded PNA as a template and its application for sensing the 5'-GCGGCGGC-3' analyte. (Reprinted with permission of [66] Copyright © 2018, American Chemical Society).

Table 1 summarizes the performances of the MIP-film-based sensors mentioned above.

Table 1. Summary of the MIP film-based SPR sensors described in Section 2.1.

Analyte	MIP Composition	Platform	Dynamic Range	Cross-Sensitivity	LOD	Ref.
Caffeine, Theophylline, Xanthine	PMMA-EGDMA ¹	SPR chip	0.4–6 mg/L	Dyphilline, Hydrochlorothiazide, Nicotin acid, phenylbutazone, Theobromide	0.4 mg/mL	[35]
PFA ²	VBT-PFDA-EDMA ²	POF-SPR ⁹	0.1–4 mg/L	nd	1.33×10^{-4} mg/mL	[39]
2-furaldehyde	MAA-DVB ³	POF-SPR ⁹	9–30 ppb	nd	9×10^{-3} mg/mL	[40,41]
TNT	MAA-DVB ³	POF-SPR ⁹	nd	2,4-dinitrotoluene, 1,3-dinitrobenzene	1.1×10^{-4} mg/mL	[42]
L-nicotine	MAA-DVB ³	POF-SPR ⁹	0–0.001 M	nd	30 mg/mL	[43]
Dibenzyl disulfide, 2-furaldehyde	MAA-DVB ³	POF-SPR ⁹	$2 \cdot 10^{-15}$ – 10^{-13} M	nd	7.24×10^{-3} mg/mL	[44]
SARS-CoV 2	Aam-TBAm-HEMA ⁴	POF-SPR ⁹	nd	nd	0.058 μ M	[45]
Amoxicillin	MAAM-VTMOs-TEOS ⁵	SPR chip	0.1–2–6 nM	Ampicillin, norfloxacin, sulfamethizole, doxycycline	73 pM	[47]
<i>S. Paratyphi</i>	MAH-HEMA-EGDMA ⁶	SPR chip	$2.5 \cdot 10^6$ – $15 \cdot 10^6$ cfu/mL	nd	1.4×10^{-6} CFU/mL	[49]
RoxP ⁷	HEMA-PEGMA ⁷	SPR chip	nd	nd	0.2 nM	[50]
Bovine serum albumin	DEAEM-BAA ⁸	SPR chip	2.5–25 nM	Human serum albumine	5.6 nM	[51]
Mycotoxin Zearalenone	Pyrrrole	SPR chip	0.3–3000 ng/L	α -zearalenol, β -zearalenol, zearalanone, and α -zearalanone	0.3 ng/g	[59]
Theophylline	TTCA ¹⁰	SPR chip	10–50 μ M	1-naphthalene sulfonic acid sodium salt, acetanilide	3.36 μ M	[60]
Paracetamol, Naproxene	TTCA ¹⁰	SPR chip	nd	caffeine, theobromine, 3-aminophenol, and 4-aminobenzoic acid	nd	[61]
Histamine	TTCA ¹⁰	SPR chip	15–500 μ g/mL	Histidine, Cadaverine, Putrescine	2 μ g/mL	[62]
Staphylococcal enterotoxin B	3-aminophenyl boronic acid	SPR chip	3.2–25.6 fM	Caffeine, Theobromine	0.05 fM	[63]
Oligonucleotides	2-(cytosin-1-yl)ethyl 4-bis(2,2'-bithien-5-yl)methylbenzoate	SPR chip	3–80 nM	nd	200 pM	[64,65]
T 2 toxin	3-aminophenyl boronic acid	SPR chip	2.1–33.6 fM	Ricin, Curcin, Arbin, MicrocistinLR	0.1 fM	[66]

¹ Polymethyl methacrylate, Ethylene glycol dimethacrylate, ² Perfluorinated alkylated substances, (Vinylbenzyl)trimethylammonium, 1H,1H,1H,2H,2H-perfluorodecyl acrylate, Ethylene dimethacrylate, ³ Methacrylic acide, Divinylbenzene. ⁴ Acrylamid, N-tert-butylacrylamide, 2-hydroxymethyl methacrylate, ⁵ Methacrylamide, vinyl-trimethoxysilane, tetraethoxysilane, ⁶ N-methacryloyl L-histidine methyl ester, 2-hydroxymethyl methacrylate, ethylene glycol dimethacrylate, ⁷ Bacterial factor, 2-hydroxymethyl methacrylate, dimethacrylate (average Mn 550), ⁸ Diethylaminoethyl methacrylate, methylenebis(acrylamide), ⁹ Plastic Optical Fiber-SPR, ¹⁰ Carboxyl functionalized-therthiophene.

2.2. NanoMIP-Based SPR Sensors

Before now, MIPs have generally been integrated into SPR sensors through a film layer. However, in recent years, attempts have been devoted to immobilizing the so-called nanoMIPs (MIP nanoparticles) onto the gold surface of the SPR chips [67–75].

For example, Sari et al. [67] proposed an SPR nanosensor for selective and rapid detection of erythromycin in aqueous solutions. Molecularly-imprinted nanoparticles were obtained by the two-phase mini-emulsion polymerization method [76] and then immobilized onto the gold surface of the SPR chip. Erythromycin is a macrolide broad spectrum antibiotic, and it was demonstrated that its residues might cause toxic effects on public health [77,78]. Hence the importance of its dosage in environmental samples. The developed sensor was applied for selectively determining erythromycin in aqueous samples. The detection limit obtained was about 0.3 mg/L. The selectivity of the nanosensor was verified in aqueous solutions containing the following competing agents: spiramycin, kanamycin sulfate, and neomycin sulfate. Tests on the repeatability of the measurements with this nanosensor have produced satisfactory results. Given the good performance, the low cost, and the rapid response, the sensor is promising for erythromycin detection in environmental waters.

The same approach was applied by Yılmaz et al. [68] to develop a nanoMIP-based SPR chip for the pesticide atrazine, by Erdem et al. [71] to realize a nanosensor for enterococcus faecalis detection, and by Rahtuvanoglu et al. [72] to develop a biosensor for histamine determination in food samples.

A rationally designed nanoMIPs coupled with an SPR sensor for detecting glycopeptide antibiotics in milk products was realized by Altintas [69] using the natural glycopeptide vancomycin as the target analyte. Figure 7 shows a scheme of the nanoMIP preparation and its immobilization on the gold surface of the SPR sensor. The nanoMIP particles were prepared by a solid phase synthesis. The prepolymeric mixture was dripped on glass beads, then a UV polymerization was carried out. Low-affinity nanoparticles were discarded by a cold wash, while those at high-affinity were collected (see Figure 7A). The obtained nanoMIPs were covalently immobilized on the gold SPR chip surface via the amine coupling reaction with the carboxylic group of the 11-mercaptoundecanoic acid (MUDA) present as a self-assembled monolayer (SAM) on the gold surface (see Figure 7B) [79]. Preliminary studies were performed with vancomycin not conjugated with gold nanoparticles (AuNPs, see Figure 7B); however, the detection limit of $50 \mu\text{g mL}^{-1}$ was insufficient to quantify trace levels of the analyte in milk samples. Consequently, to increase the sensor's sensitivity, vancomycin was conjugated with AuNPs, obtaining a detection limit of 4.1 ng mL^{-1} and a linear concentration range from 10 to 125 ng mL^{-1} . The great selectivity was verified by comparative investigations with nanoMIPs and nanoNIPs. Cross-reactivity tests with other drugs demonstrated the high specificity of the sensor towards the target analyte vancomycin. The coupling of the nanoMIPs with SPR chips once again proved the potentiality of these sensors for a cheap, reliable, and rapid detection of contaminants in environmental and biological samples.

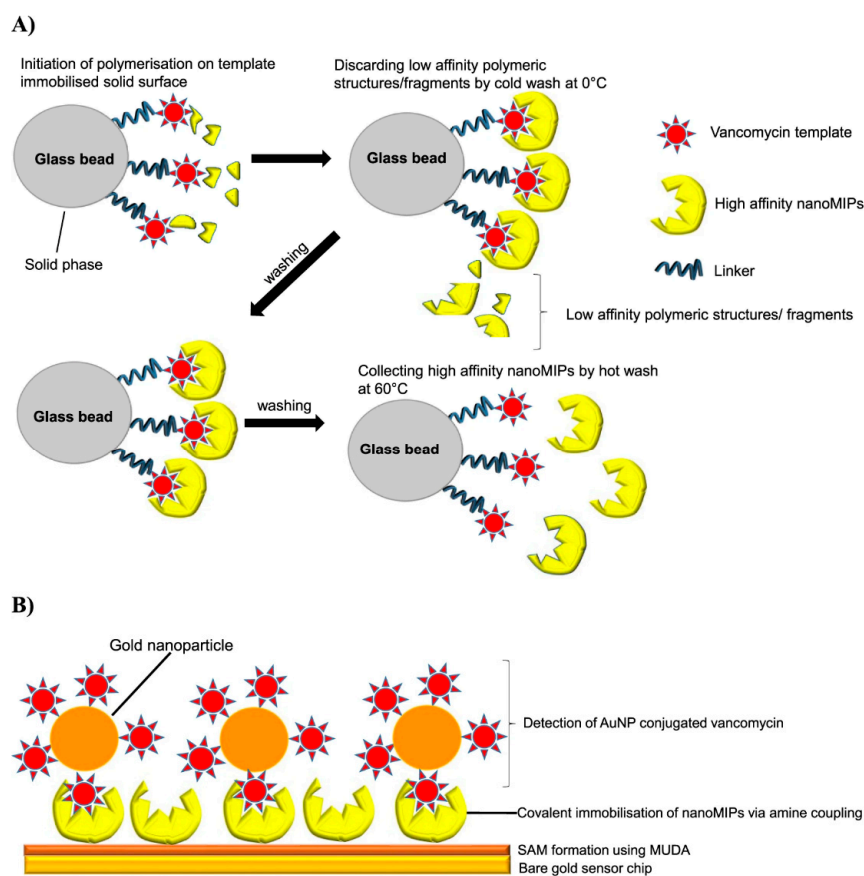


Figure 7. (A) Scheme of the preparation of vancomycin nanoMIP. (B) Scheme of the nanoMIP immobilization on the gold surface of the SPR chip. (Reproduced with permission from [69], open access Creative Common CC licensed 4.0, Springer Nature).

Similar nanoMIPs synthesis and immobilization technique were used by Ashley et al. to develop an SPR nanosensor for α -casein detection in milk samples [70].

Cennamo et al. [73–75] developed plasmonic biosensors combined with deformable nanoMIPs prepared by exploiting the hydrogel synthesis by precipitation-polymerization in solution [80]. The mild conditions of this precipitation-polymerization employing acrylamides were necessary for imprinting biomacromolecules. The nanoMIPs synthesis involved acrylamide (Aam), methacrylic acid (MAA), and N-t-butylacrylamide (TBAm) as functional monomers. N, N-methylenebisacrylamide (BIS) was used as a cross-linker and a mix of ammonium persulfate and N,N,N,N-tetramethylethylenediamine was employed as the polymerization initiator.

In [73], nanoMIPs for sensing human serum transferrin (HTR) were synthesized. Plastic optical fiber (POF) was used to develop a D-shaped POF SPR platform. When coupled to the POF-SPR platform, the nanoMIPs deformations induced by the interaction with the analyte amplified the resonance shift, allowing the HTR detection with ultra-low sensitivity. Indeed, the realized sensor responded linearly in the HTR concentration range from 1.2 fM to 1.8 pM with a detection limit of 1.2 fM.

A nanoplasmonic sensor chip was proposed in [74]. It was based on gold nanograting realized on a PMMA substrate and faced with soft nanoMIPs for selective recognition of Bovine Serum Albumin (BSA). Even in this case, the characteristic deformable properties of the nano-MIPs enabled a significant enhancement of the biosensor's detection limit (LOD of about 3 fM).

The most recent sensor is that proposed in [75]. The paper described the development of an SPR platform using silica light-diffusing fibers (LDFs) functionalized with nanoMIPs for detecting the protein human serum transferrin (HTR). Figure 8 shows a scheme of the sensor's operating principle.

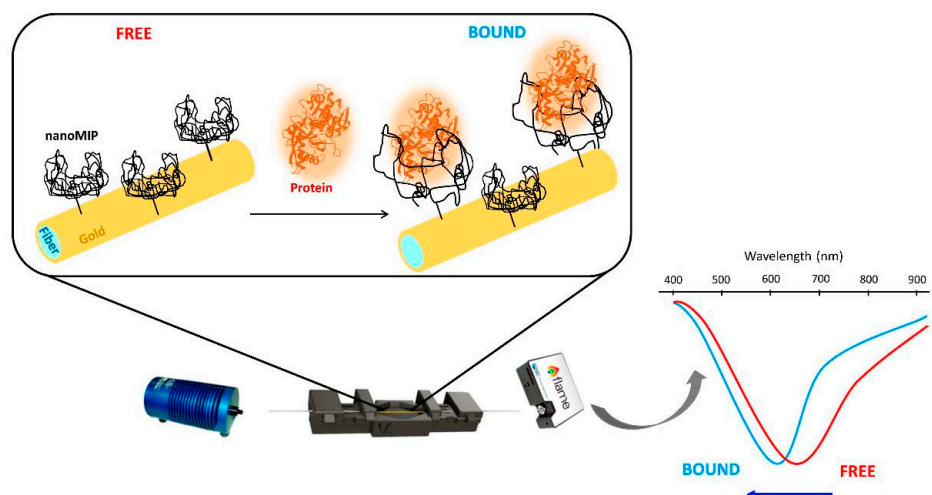


Figure 8. Scheme of the operating principle of the nanoMIPs-based SPR-LFD platform for HTR detection. (Reproduced with permission from [75], open access Creative Common CC licensed 4.0, MDPI).

The innovative approach of combining an SPR-LFD platform with nanoMIPs permitted the realization of a selective sensor with an ultra-low detection limit for HTR of about 4 fM. The main advantage of this kind of chip is the simpler fabrication. Indeed, the sensor preparation required only a gold nanolayer deposition on the LDF, opening the opportunity to scale up the production of these devices for different analytes.

The above-described devices are summarized in Table 2.

Table 2. Summary of the nanoMIP-based SPR sensors described in Section 2.2.

Analyte	MIP Composition	Polymerization Method	Platform	LOD	Dynamic Range	Cross Sensitivity	Ref.
Erythromycin	MAA-EGDMA-HEMA ¹	Two-phase mini-emulsion polymerization	SPR-CHIP	0.3 mg/L	$(6.8-68.1) \times 10^{-6}$ mol dm ⁻³	nd	[67]
Atrazine	MAA-EGDMA-HEMA ¹	Two-phase mini-emulsion polymerization	SPR-CHIP	0.7134 ng/mL	0.5–1.5 ng mL ⁻¹	Simazine, Amitrole	[68]
Glycopeptide antibiotics	EGDMA-TRIM ²	Solid phase synthesis	SPR-CHIP	4.1 ng/L	10–200 µg Kg ⁻¹	Teicoplanin, Artemisinin	[69]
α-Casein	NIPAm-BIS-APM-TBAm-AA ³	Solid phase synthesis	SPR-CHIP	127 ng/mL	0.5–8 ppm	BLG ⁸ , BSA ⁹	[70]
Enterococcus faecalis	MAH-HEMA-EGDMA ⁴	Two-phase mini-emulsion polymerization	SPR-CHIP	1.05×10^2 cfu/mL	$2 \times 10^4-1 \times 10^8$ cfu mL ⁻¹	<i>E. coli</i> , <i>B. subtilis</i> , <i>S. aureus</i>	[71]
Histamine	MAH-HEMA-EGDMA ⁴	Two-phase mini-emulsion polymerization	SPR-CHIP	0.58 ng/mL	0.001–10 µg mL ⁻¹	Histidine, Tryptophan, Dopamine	[72]
HTR ⁵	Aam-MAA-TBAm-BIS ⁶	Solution precipitation polymerization	POF-SPR ⁷	1.2 fM	1.2 fM–1.8 pM	nd	[73]
BSA	AaM-MAA-TBAm-BIS ⁶	Solution precipitation polymerization	POF-SPR ⁷	3 fM	2 fM–0.1 pM	α-lactalbumin, myoglobin	[74]
HTR	AaM-MAA-TBAm-BIS ⁶	Solution precipitation polymerization	POF-SPR ⁷	4 fM	8–280 fM	PEP, HRP	[75]

¹ Methacrylic acid, Ethylene glycol dimethacrylate, 2-hydroxyethyl methacrylate, ² Ethylene dimethacrylate, Trimethylpropane trimethacrylate, ³ N-Isopropylacrylamide, N,N-methylenebis(acrylamide), N-(3-aminopropyl)methacrylamide, N-tert-butylacrylamide, acrylic acid, ⁴ N-methacryloyl-(L)-histidine-methylester, 2-hydroxyethyl methacrylate, Ethylene glycol dimethacrylate, ⁵ Human Serum Albumin Acrylamide, Methacrylic acid, N-t-butylacrylamide, N,N'-methylenebisacrylamide, ⁶ Acrylamide, Methacrylic acid, N-t-butylacrylamide, N,N'-methylenebisacrylamide, ⁷ Plastic Optical Fiber-SPR, ⁸ β-Lactoglobulin, ⁹ Bovine serum albumin.

2.3. MIP-Coated Nanoparticles-Based LSPR and SPR Sensors

Recent progress in nano-optics allowed the development of sensors based on LSPR signals of nanostructures. LSPR is produced by light when it interacts with metal nanoparticles with dimensions smaller than the incident wavelength. As in SPR, when the surface plasmons are confined to a nanoparticle with a size comparable to or less than the light wavelength, coherent localized plasmon oscillations occur with a resonant frequency dependent on the composition, size, geometry, separation distance of nanoparticles, and surrounding dielectric medium [81,82].

Gold nanoparticles (AuNPs) have been intensely studied in the past decade thanks to their remarkable properties, which make them helpful in developing sensors and biosensors. However, AuNPs alone are often unsuitable for sensing applications. Modifying their surface with inorganic or organic functionalities is essential to improve stability and selectivity. Among the recognition receptors, MIPs are of particular interest since their characteristics of merit include easy synthesis, high stability, and low cost. Hybrid structures obtained by coupling AuNPs with MIPs represent the new trend in developing plasmonic sensors with high sensitivity and specificity [83]. Moreover, MIP-based LSPR sensors are compatible with microfluidic systems, reducing the size and making the optical devices portable and available for in situ and point-of-care analyses [84].

The first surface-imprinted LSPR sensor based on gold nanorods for protein detection was proposed by Abbas et al. in 2013, employing a sol-gel synthesis and using siloxane copolymerization [85]. A scheme of the nanosensor preparation is shown in Figure 9.

Neutrophil gelatinase-associated lipocalin (NGAL), a biomarker for acute kidney injury, was employed as a target template for a proof of concept development of the sensor. LSPR activity of the imprinted nanorods enabled the monitoring of the imprinting process and also the detection of the protein capture and release at physiological concentrations. The good results opened a new perspective on MIP-based LSPR nanosensors for biomedical applications as diagnostic tools.

More recently, Hu et al. synthesized a shell of a sol-gel MIP on gold nanorods for target proteins to investigate the role of aromatic interactions in molecular recognition [86]. As template molecules, three proteins with different aromatic amino acid functionalities were selected. MIPs were prepared on gold nanorods using monomers of diverse aromatic groups. The results showed a protein-dependent enhancement of selectivity and sensitivity due to the presence of aromatic functionalities in the imprinted polymer network.

Higher enhancement in sensitivity was found for proteins with more aromatic amino acid groups, highlighting the need for a fine selection of functional monomers in synthesizing molecularly imprinted polymers.

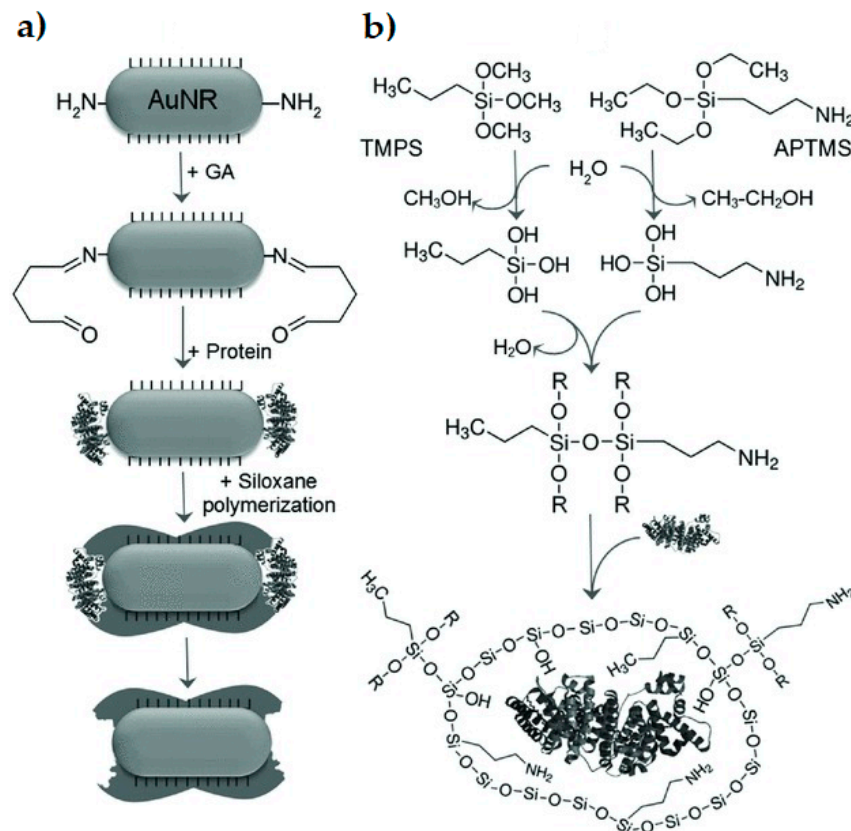


Figure 9. Preparation of the MIP-based LSPR nanosensor by imprinting gold nanorods. (a) molecular imprinting steps: attachment of p-ATP to the ends of the gold nanorod; glutaraldehyde (GA) interaction with the amine groups of p-ATP on one side and with the amine groups of the protein on the other side; siloxane monomers polymerization in the presence of the protein templates. The release of the protein results in recognition cavities. (b) copolymerization of the organo-siloxane monomers APTMS and TMPS. (Reproduced with permission from [85], Copyright © 2013 WILEY-VCH).

Guerreiro et al. proposed an LSPR sensor to evaluate wine astringency as an alternative method to sensorial analysis [87]. In particular, the nanosensor combined LSPR with surface-modified gold nanodisks by molecularly imprinted polymers. The study aimed to simulate astringency, determined by the tannins of the wine, in the mouth by imitating the biological system. For the gold nanodisks' surface modification by molecular imprinting, salivary proteins were used as template molecules, thiophenecarboxylic acid, (vinylbenzyl)trimethylammonium and methacrylic acid as functional monomers, and EGDMA acted as a cross-linker. The sensor's response was expressed in pentagalloyl glucose (PGG) units and the linearity was verified from 1 to 140 $\mu\text{mol/L}$ PGG. The sensor was also applied to wine samples demonstrating a good agreement with the data obtained by sensorial analysis. The correlation between astringency and wine composition was also assessed, highlighting the role of anthocyanins in pigmentation and astringency.

An LSPR biosensor based on hydrogel-coated silica core-gold nanoshells was proposed by Culver et al. for the detection of protein biomarkers of chronic dry eyes, such as lactoferrin and lysozyme [88]. Poly(N-isopropylacrylamide-co-methacrylic acid) hydrogel acted as molecular recognition units for the target proteins. Lactoferrin and lysozyme exhibit a high isoelectric point, so electrostatic interaction with the negatively charged units in the hydrogel and the positively charged proteins occurred. This interaction provoked a

red shift in the LSPR wavelength, increasing alongside the increase of protein concentration. Figure 10 depicts a scheme of the sensing mechanism. The developed biosensor is promising for screening both protein biomarkers of chronic dry eyes.

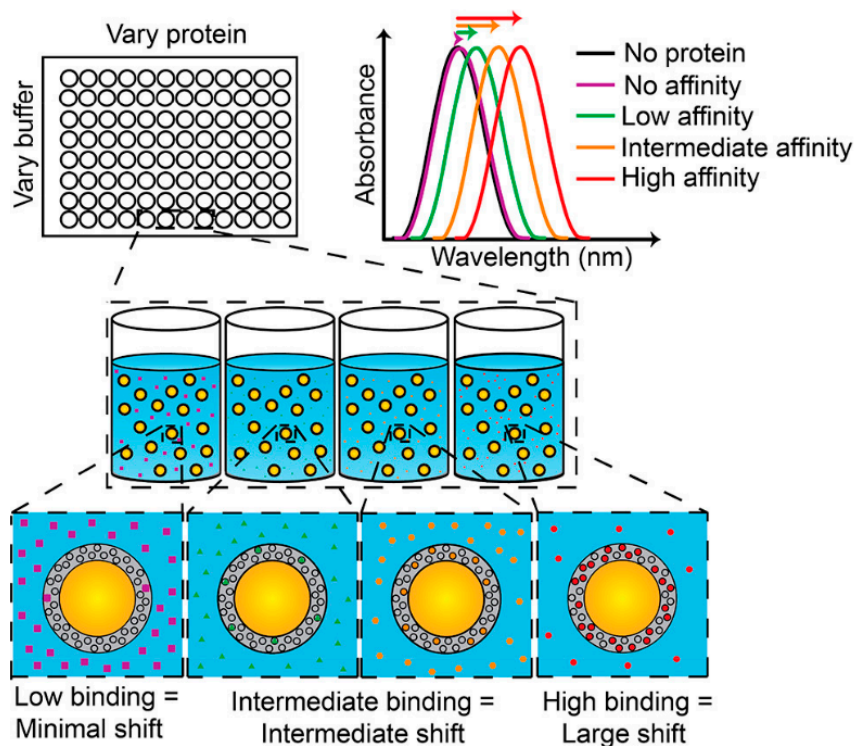


Figure 10. Scheme of the LSPR biosensor based on hydrogel-coated silica core-gold nanoshells. The shift in LSPR depends on protein concentration and affinity for the recognition units. (Reprinted with permission of [88] Copyright © 2018, American Chemical Society).

MIP-based LSPR gas sensors were also developed by the group of Prof. Hayashi [89,90].

MIP-coated gold nanoparticles were applied for LSPR sensing of α -pinene vapor [89]. α -pinene is a monoterpene that can be emitted by paper and pulp industries and fragrance manufacturers. Its reaction in the atmosphere produces particulates that form a blue haze and reduce visibility. Moreover, free radicals are formed which are responsible for the depletion of the ozone layer. α -pinene vapor becomes a human nuisance due to its intense odor [91–94]. Therefore, its detection is very important. The sensor developed in [89] was obtained by covering gold nanoparticles with a molecularly imprinted polymer film prepared with α -pinene as the template, methacrylic acid as the functional monomer, and ethylene glycol dimethyl acrylate as the cross-linker. A red shift of the nanoparticles' plasmon absorbance peak occurred thanks to the MIP's coating, proportional to α -pinene vapor concentration. LSPR response was verified to be reproducible, reversible, and rapid.

The same authors also proposed a nanocomposite-imprinted LSPR sensor for volatile cis-jasmone in plants. Detecting this volatile compound allows for monitoring plants' growth pressure, which is especially helpful in sensing attacks by herbivores. The sensor was prepared by spin-coating titanium molecularly imprinted sol-gel onto gold nanoislands, as shown in Figure 11.

The gas molecules were detected by monitoring the variations in absorption spectra of the MIP-modified gold nanoislands due to the refractive index variation, according to the LSPR phenomenon. The detection limit obtained was 3.5 ppm. The good performances of the sensor were promising for its application to determine cis-jasmone in agriculture.

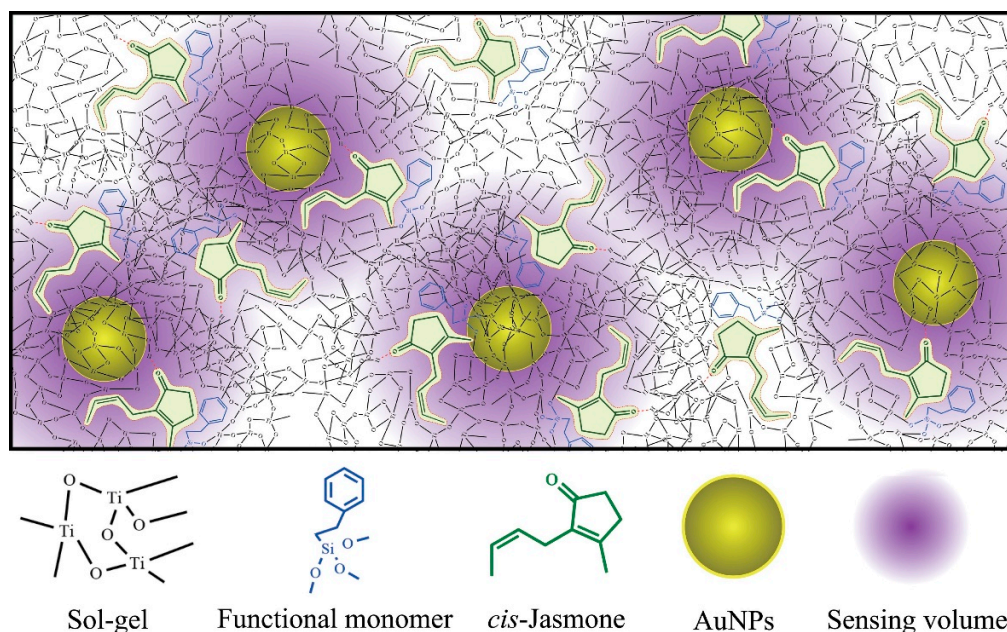


Figure 11. Scheme of the MIP-coated gold nanoislands with functional monomers for *cis*-jasmone vapor detection. (Reprinted with permission of [90] Copyright © 2018, Elsevier B.V.).

Chegel et al. proposed MIP-based LSPR nanochips for explosives analogs detection in vapor and liquid phases [95]. The approach focused on the development of nanochips consisting of a random array of gold nanoislands immobilized on glass slides. For obtaining the MIP coating, the gold nanochip surface was first functionalized with a monolayer of 3-mercaptopropyl(diethyl)carbamo-dithioate as an initiator of UV polymerization. Then, the UV-induced polymerization was performed using an acrylamide functional monomers mixture and the explosive analog 4-nitrophenol as a template. 4-nitrophenol was employed since its similar structure to that of trinitrotoluene (TNT) explosive. A detection limit of 1 pM in the aqueous phase and 0.1 ppm in the gaseous state was achieved. The nanochip demonstrated some degree of selectivity, being sensitive to explosive analogs with structures similar to the template (1-nitronaphthalene, 5-nitroisoquinoline, and 4-nitrotoluene). Optimization of the sensors has to be done, in particular, to improve the molecular imprinting synthesis to increase the number of recognition cavities and tune the thickness of the polymer to enhance selectivity and response time.

Recently, Wang et al. developed an LSPR biosensor based on a polydopamine MIP for enrofloxacin residues detection in chicken meat [96]. The target analyte is a fluoroquinolone antibiotic of a broad antibacterial spectrum, classified as an emergent contaminant. Consequently, selective and sensitive methods for enrofloxacin determination are crucial [96–99]. The polydopamine-based MIP film was prepared in an aqueous solution by self-polymerization at room temperature with a mixture of dopamine as the functional monomer and enrofloxacin as the template. To amplify LSPR signals, conjugates with a protein (bovine serum albumin) were prepared and used in competing tests. The time of analysis was about 20 min. The sensor responded to enrofloxacin in a detection range from 25 to 1000 ng/mL with a detection limit equal to 61 ng/mL. The reusability was also verified, and the sensor can be regenerated seven times without losing performance. The MIP-modified chip was applied to detect the target analyte in spiked chicken meat samples obtaining good recovery (between 80 and 95%). Thanks to the high sensitivity, stability, and selectivity, the developed biosensor is promising for in situ analysis of enrofloxacin residues in food and environmental samples.

Table 3 summarizes the nanosensors described in this paragraph.

Table 3. Summary of the MIP-coated nanoparticles-based LSPR sensors described in Section 2.3.

Analyte	MIP Composition	Polymerization Method	Nanoobjects	LOD	Dynamic Range	Cross-Selectivity	Ref.
Proteins	TMPS-APTMS ¹	Sol-Gel	Au nanorods	0.32 µg/mL	0.25 nM–16 µM	Hemoglobin, BSA ⁶	[85]
Aromatic proteins	TMPS-APTMS-TMPHs ²	Shell Sol-Gel	Au nanorods	0.5 µg/mL	0.9–1.5 nM	HAS ⁷ , BSA ⁶	[86]
Polyphenols	TPCA-MAA-EGDMA-MA ³	Surface polymerization	Au nanodisks	1 µM	1–100 µM	nd	[87]
Lactoferrin Lysozyme	PNM ⁴	Hydrogel	Silica core-Au nanoshells	32 µg/mL	nd	nd	[88]
α-pinene vapor	MAA-EGDMA ⁵	Bulk polymerization	Gold nanoparticles	0.8 ppm	3.8–46.4 ppm	nd	[89]
Explosives	Acrylamide mixture	Surface polymerization	Gold nanoislands	1 pM water 0.1 ppm vapor	1 pM–100 µM	nd	[95]
Enrofloxacin	Polydopamine	Self bulk polymerization	Gold nanoparticles chip	61 ng/mL	0–100 ng/mL	DANO ⁸ , TETR ⁹ , PHTH ¹⁰	[96]

¹ Trimethoxypropylsilane, (3-aminopropyl)trimethoxysilane, ² Trimethoxypropylsilane, (3-aminopropyl)trimethoxysilane, Trimethoxyphenylsilane, ³ Thiophenecarboxylic acid, Methacrylic acid, Ethylene glycol dimethacrylate, Methyl acrylate, ⁴ poly(N-isopropylacrylamide-co-methacrylic acid), ⁵ Methacrylic acid, Ethylene glycol dimethacrylate, ⁶ Bovine serum albumin, ⁷ Human serum albumin, ⁸ Danofloxacin, ⁹ Tetracycline, ¹⁰ Phthalic acid.

The localized plasmon of metal nanoparticles, particularly those of gold and silver, were extensively used to amplify SPR signals. The coupling of the nanoparticles' localized plasmon with the surface plasmon wave affects the plasmon energy and, consequently, the enhancement of the SPR shifts occurs [100].

For example, Frascioni et al. [101] proposed an SPR sensor for antibiotics obtained by synthesizing gold nanoparticles modified with a capping monolayer of the electropolymerizable thioaniline units and phenylboronic acid ligands. After electropolymerization on the SPR gold surface of the functionalized nanoparticles in the presence of the target antibiotic as the template, molecularly-imprinted recognition sites were obtained. The obtained sensor was applied to antibiotics detection in milk samples with good performances in terms of low detection limit (200 fM), high selectivity, and sensitivity.

The same approach was applied to develop SPR sensors for the selective detection of amino acids, in particular for a chiroselective determination of glutamic acid [102]. By co-functionalizing the thioaniline-modified gold nanoparticles with cysteine units, electropolymerizable AuNPs able to bind amino acids through complementary zwitterionic interactions were produced, enabling the synthesis of imprinted materials for different amino acids.

Additionally, an analogous procedure was employed for developing SPR sensors for enantioselective detection of mono- and disaccharides [103].

An AuNPs-decorated MIP-based SPR sensor to detect Aflatoxin M1 in milk samples was recently proposed [104,105]. The AuNPs were functionalized with MIP nanofilm and linked to the gold surface of the SPR chip previously coated with allyl mercaptan. For the MIP synthesis, N-methacryloyl-L-phenylalanine was selected as a functional monomer, ethylene glycol dimethacrylate as a cross-linker, and Aflatoxin M1 as the template. A detection limit of 0.4 pg/mL and a good linear range (between 0.0003 ng/mL and 20.0 ng/mL) was achieved, demonstrating the promising performance of the sensor.

Selective and sensitive detection of the neurotransmitter dopamine in aqueous solutions and biological samples was obtained by MIP-functionalized AuNPs on the surface of an SPR sensor [106]. N-Methacryloyl-(L)-cysteine methyl ester and N-methacryloyl-(L)-phenylalanine methyl ester were employed as functional monomers, and 2-hydroxyethyl methacrylate and ethyleneglycol dimethacrylate were the cross-linkers. This SPR biosensor could be a potential alternative to existing methods for dopamine determination thanks to the ease and cost of preparation, low solvent consumption, small sample amount, and rapid analysis time.

Table 4 summarizes the performances of the over-cited AuNPs-decorated MIP-based SPR sensors.

Table 4. Summary of the AuNPs-decorated MIP-based SPR sensors described in Section 2.3.

Analyte	MIP Composition	Platform	Dynamic Range	Cross Sensitivity	LOD	Ref.
Noemycin, Kanamycin, Streptomycin, Enrofloxacin	Thioaniline	SPR chip	2×10^{-6} –20 nM	nd	200 fM	[101]
Amino acids	Thioaniline-cysteine	SPR chip	0.002–4 μ M	nd	2 nM	[102]
Mono-, disaccharides	Boronic acid	SPR chip	10^{-6} –200 nM	nd	40 ppb	[103]
Aflatoxin M1	N-methacryloyl-L-phenylalanine	SPR chip	0.0003–20 ng/mL	Aflatoxin B1, citrinin, ochratoxin A	0.4 pg/mL	[104,105]
Dopamine	N-Methacryloyl-(L)-cysteine methyl ester, N-methacryloyl-(L)-phenylalanine methyl ester	SPR chip	0.01–0.075 ppb 0.15–0.5 ppb	(\pm)-epinephrine hydrochloride, L-norepinephrine hydrochloride	0.091 ppb	[106]

2.4. MIP-Based SPR Imaging Sensors

MIP-based SPR imaging sensors employ a surface-sensitive optical technique to detect two-dimensional spatial phase variation due to the sorption of biomolecules on a sensing surface obtained by highly-selective MIPs films [107]. SPR imaging permits multiple analyte detection thanks to the multiple MIP-film sensing spots on the SPR chip.

In 2006, Lee et al. proposed a microfluidic chip integrated with an array of MIP films for SPR imaging of specific bioanalytes [107]. The microfluidic chip was fabricated using micro-electro-mechanical-system technology and comprised of micropumps/microvalves, microchannels, and a micromachine-based temperature control system. The MIP films were prepared using methacrylic acid as the functional monomer, divinylbenzene as a cross-linker, and progesterone, cholesterol, and testosterone as templates. Pre-polymeric mixtures were spin-coated on the SPR gold surface and UV polymerization was carried out. The developed MIP-based SPR microfluidic chip could be promising for nano-sensing applications and for detecting biomolecules at a low molecular weight.

Lautner et al. presented micropatterned surface-imprinted polymers for protein recognition obtained by photolithographic technique [108]. Avidin-imprinted poly(3,4-ethylenedioxythiophene)/poly(styrenesulfonate) conducting polymer microbands were prepared directly on the SPR chip surface. The interaction of the micropatterns MIPs' cavities with the protein was determined straightforwardly with SPR imaging with sensitivity comparable to or higher than fluorescence imaging.

Microelectrospotting for electrodeposition of MIP microarrays on the gold surface of SPR imaging chips was proposed by Bossert et al. [109] for protein analysis. The spotting pin surrounded the monomer-template (protein) mixture that, after contact with the gold surface, was in-situ electropolymerized forming spots of about 500 μ m diameter. As a proof-of-concept of the procedure, scopoletin was employed as the monomer and ferritin as the template. It was demonstrated that microelectrospotting of MIPs combined with SPR imaging could be a versatile platform for label-free protein recognition and analytical determination.

Luo et al. proposed an SPR imaging chip with a MIP array fabricated through step-by-step polymerization using a photomask [110] for multiplex antibiotics detection. An SPR analysis of two different antibiotics (ciprofloxacin and azithromycin) was performed, obtaining a specific cross-reactive response pattern to ciprofloxacin and azithromycin, demonstrating the feasibility of the employed technology for multiplex analyte detection.

Table 5 summarizes the figures of merits of the above-described sensors.

Table 5. Summary of the MIP-based SPR imaging (SPRi) sensors described in Section 2.4.

Analyte	MIP Composition	Platform	Dynamic Range	Cross Sensitivity	LOD	Ref.
Progesterone, cholesterol, testosterone	Methacrylic acid	SPRi chip	nd	nd	0.1 μ M	[107]
Proteins	poly(3,4-ethylenedioxythiophene)/poly(styrenesulfonate)	SPRi chip	8×10^{-4} –0.5 mg/mL	Streptavidin, neutravidin, and extravidin	125 nM	[108]
Proteins	Scopoletin	SPRi chip	nd	nd	nd	[109]
Enrofloxacin	Itaconic acid	SPRi chip	0.15–20 μ g/L	Ciprofloxacin, ofloxacin, azithromycin, dopamine, penicillin	0.3 μ g/L	[110]
Sulfapyridine					0.29 μ g/L	
Chloramphenicol					0.26 μ g/L	

3. Conclusions

The MIP-based plasmonic sensors discussed in the present review highlight the demand for devices for high sample throughput analysis avoiding time-consuming sample preparation techniques and bulky, expensive methods.

In recent years, the development of MIP-based plasmonic chemosensors and biosensors for a wide range of applications has significantly increased. The main advantages of MIP-based plasmonic platforms include very low detection limits, high sensitivity and selectivity, rapid responses, and low-cost instrumentations.

However, some drawbacks must be solved, like enhancement of reproducibility, sensitivity improvement, and the expansion MIP-based plasmonic sensors to a wide range of sectors. Improving reproducibility is essential for the enhancement of the sensors' performance. On the other end, effort must be committed to overcoming some MIPs' weaknesses, like the irregular shape of the polymer, heterogeneous bead sizes, and unspecific cavities.

Unfortunately, to date, MIP-based sensors are studied and developed only at the academic level and their applications remain at the proof-of-concept stage.

Given the advantages of these sensors, such as the high selectivity and sensitivity, potential for miniaturization, and quick responses, practical applications in different fields should be assumed.

Author Contributions: Conceptualization, G.A.; writing—original draft preparation, G.A. and C.Z.; writing—review and editing, S.S., L.R.M. and R.B. All authors have read and agreed to the published version of the manuscript.

Funding: This research received no external funding.

Data Availability Statement: Not applicable.

Conflicts of Interest: The authors declare no conflict of interest.

References

1. Lowdon, J.W.; Diliën, H.; Singla, P.; Peeters, M.; Cleij, T.J.; van Grinsven, B.; Eersels, K. MIPs for commercial application in low-cost sensors and assays—An overview of the current status quo. *Sens. Actuators B Chem.* **2020**, *325*, 128973. [[CrossRef](#)]
2. Dickert, F.L. Molecular imprinting and functional polymers for all transducers and applications. *Sensors* **2018**, *18*, 327. [[CrossRef](#)] [[PubMed](#)]
3. Uzun, L.; Turner, A.P.F. Molecularly-imprinted polymer sensors: Realizing their potential. *Biosens. Bioelectron.* **2016**, *76*, 131–144. [[CrossRef](#)] [[PubMed](#)]
4. Hayden, O. One binder to bind them all. *Sensors* **2016**, *16*, 1665. [[CrossRef](#)]
5. Hayden, O.; Lieberzeit, P.A.; Blaas, D.; Dickert, F.L. Artificial antibodies for bioanalyte detection—Sensing viruses and proteins. *Adv. Funct. Mater.* **2006**, *16*, 1269–1278. [[CrossRef](#)]
6. Ye, L.; Haupt, K. Molecularly imprinted polymers as antibody and receptor mimics for assays, sensors and drug discovery. *Anal. Bioanal. Chem.* **2004**, *378*, 1887–1897. [[CrossRef](#)]
7. Leibl, N.; Haupt, K.; Gonzato, C.; Duma, L. Molecularly Imprinted Polymers for Chemical Sensing: A Tutorial Review. *Chemosensors* **2021**, *9*, 123. [[CrossRef](#)]
8. Chen, L.; Wang, X.; Lu, W.; Wu, X.; Li, J. Molecular imprinting: Perspectives and applications. *Chem. Soc. Rev.* **2016**, *45*, 2137–2211. [[CrossRef](#)] [[PubMed](#)]
9. Bedwell, T.S.; Whitcombe, M.J. Analytical applications of MIPs in diagnostic assays: Future perspectives. *Anal. Bioanal. Chem.* **2016**, *408*, 1735–1751. [[CrossRef](#)]
10. Piletsky, S. *Molecular Imprinting of Polymers*, 1st ed.; CRC Press: Boca Raton, FL, USA, 2006.
11. Murdaya, N.; Triadenda, A.L.; Rahayu, D.; Hasanah, A.N. A Review: Using Multiple Templates for Molecular Imprinted Polymer: Is It Good? *Polymers* **2022**, *14*, 4441. [[CrossRef](#)]
12. Vasapollo, G.; del Sole, R.; Mergola, L.; Lazzoi, M.R.; Scardino, A.; Scorrano, S.; Mele, G. Molecularly Imprinted Polymers: Present and Future Prospective. *Int. J. Mol. Sci.* **2011**, *12*, 5908–5945. [[CrossRef](#)]
13. Asman, S.; Mohamad, S.; Sarih, N.M. Exploiting β -Cyclodextrin in Molecular Imprinting for Achieving Recognition of Benzylparaben in Aqueous Media. *Int. J. Mol. Sci.* **2015**, *16*, 3656–3676. [[CrossRef](#)]
14. Zaidi, S.A. Molecular imprinted polymers as drug delivery vehicles. *Drug Deliv.* **2014**, *23*, 2262–2271. [[CrossRef](#)]
15. Pardo, A.; Mespouille, L.; Dubois, P.; Blankert, B.; Duez, P. Molecularly Imprinted Polymers: Compromise between Flexibility and Rigidity for Improving Capture of Template Analogues. *Chem. A Eur. J.* **2014**, *20*, 3500–3509. [[CrossRef](#)] [[PubMed](#)]
16. Caro, E.; Marce, R.; Borrull, F.; Cormack, P.; Sherrington, D. Application of molecularly imprinted polymers to solid-phase extraction of compounds from environmental and biological samples. *TrAC Trends Anal. Chem.* **2006**, *25*, 143–154. [[CrossRef](#)]

17. Sanagi, M.M.; Salleh, S.; Ibrahim, W.A.W.; Abu Naim, A.; Hermawan, D.; Miskam, M.; Hussain, I.; Aboul-Enein, H.Y. Molecularly imprinted polymer solid-phase extraction for the analysis of organophosphorus pesticides in fruit samples. *J. Food Compos. Anal.* **2013**, *32*, 155–161. [[CrossRef](#)]
18. Kadhem, A.J.; Gentile, G.J.; Fidalgo de Cortalezzi, M.M. Molecularly Imprinted Polymers (MIPs) in Sensors for Environmental and Biomedical Applications: A Review. *Molecules* **2021**, *26*, 6233. [[CrossRef](#)]
19. Ahmad, O.S.; Bedwell, T.S.; Esen, C.; Garcia-Cruz, A.; Piletsky, S.A. Molecularly imprinted polymers in electrochemical and optical sensors. *Trends Biotechnol.* **2019**, *37*, 294–309. [[CrossRef](#)]
20. Maier, S.A. *Plasmonics: Fundamentals and Applications*; Springer-Verlag: New York, NY, USA, 2007; pp. 21–34.
21. Daghestani, H.N.; Day, B.W. Theory and Applications of Surface Plasmon Resonance, Resonant Mirror, Resonant Waveguide Grating, and Dual Polarization Interferometry Biosensors. *Sensors* **2010**, *10*, 9630–9646. [[CrossRef](#)]
22. Chen, Y.; Ming, H. Review of surface plasmon resonance and localized surface plasmon resonance sensor. *Photonic Sens.* **2012**, *2*, 37–49. [[CrossRef](#)]
23. Boozer, C.; Kim, G.; Cong, S.; Guan, H.; Londergan, T. Looking towards label-free biomolecular interaction analysis in a high-throughput format: A review of new surface plasmon resonance technologies. *Curr. Opin. Biotechnol.* **2006**, *17*, 400–405. [[CrossRef](#)]
24. Esen, C.; Piletsky, S.A. Surface Plasmon Resonance Sensors Based on Molecularly Imprinted Polymers. In *Plasmonic Sensors and Their Applications*; Denizli, A., Ed.; Wiley-VCH GmbH: Weinheim, Germany, 2021; Chapter 13; pp. 221–235.
25. Mayer, K.M.; Hafner, J.H. Localized surface plasmon resonance sensors. *Chem. Rev.* **2011**, *111*, 3828–3857. [[CrossRef](#)] [[PubMed](#)]
26. Verellen, N.; Van Dorpe, P.; Huang, C.; Lodewijks, K.; Vandenbosch, G.A.; Lagae, L.; Moshchalkov, V.V. Plasmon line shaping using nanocrosses for high sensitivity localized surface plasmon resonance sensing. *Nano Lett.* **2011**, *11*, 391–397. [[CrossRef](#)] [[PubMed](#)]
27. Liu, J.; Jalali, M.; Mahshid, S.; Wachsmann-Hogiu, S. Are plasmonic optical biosensors ready for use in point-of-need applications? *Analyst* **2020**, *145*, 364–384. [[CrossRef](#)]
28. Gupta, B.D.; Shrivastav, A.M.; Usha, S.P. Surface Plasmon Resonance-Based Fiber Optic Sensors Utilizing Molecular Imprinting. *Sensors* **2016**, *16*, 1381. [[CrossRef](#)] [[PubMed](#)]
29. Arghir, I.; Delpont, F.; Spasic, D.; Lammertyn, J. Smart design of fiber optic surfaces for improved plasmonic biosensing. *N. Biotechnol.* **2015**, *32*, 473–484. [[CrossRef](#)] [[PubMed](#)]
30. Qu, J.H.; Dillen, A.; Saeys, W.; Lammertyn, J.; Spasic, D. Advancements in SPR biosensing technology: An overview of recent trends in smart layers design, multiplexing concepts, continuous monitoring and in vivo sensing. *Anal. Chim. Acta* **2020**, *1104*, 10–27. [[CrossRef](#)] [[PubMed](#)]
31. Cennamo, N.; Pesavento, M.; Zeni, L. A review on simple and highly sensitive plastic optical fiber probes for bio-chemical sensing. *Sens. Actuators B Chem.* **2021**, *331*, 129393. [[CrossRef](#)]
32. Yang, W.; Ma, Y.; Sun, H.; Huang, C.; Shen, X. Molecularly imprinted polymers based optical fiber sensors: A review. *TrAC Trends Anal. Chem.* **2022**, *152*, 116608. [[CrossRef](#)]
33. Chiappini, A.; Pasquardini, L.; Bossi, A.M. Molecular Imprinted Polymers Coupled to Photonic Structures in Biosensors: The State of Art. *Sensors* **2020**, *20*, 5069. [[CrossRef](#)]
34. Fang, L.; Jia, M.; Zhao, H.; Kang, L.; Shi, L.; Zhou, L.; Kong, W. Molecularly imprinted polymer-based optical sensors for pesticides in foods: Recent advances and future trends. *Trends Food Sci. Technol.* **2021**, *116*, 387–404. [[CrossRef](#)]
35. Lai, E.P.C.; Fafara, A.; Noot, V.A.V.; Kono, M.; Polsky, B. Surface plasmon resonance sensors using molecularly imprinted polymers for sorbent assay of theophylline, caffeine, and xanthine. *Can. J. Chem.* **1998**, *76*, 265–273. [[CrossRef](#)]
36. Rico-Yuste, A.; Carrasco, S. Molecularly imprinted polymer-based hybrid materials for the development of optical sensors. *Polymers* **2019**, *11*, 1173. [[CrossRef](#)]
37. Chen, B.; Liu, C.; Xie, Y.; Jia, P.; Hayashi, K. Localized surface plasmon resonance gas sensor based on molecularly imprinted polymer coated au nanoisland films: Influence of nanostructure on sensing characteristics. *IEEE Sensors J.* **2016**, *16*, 3532–3540. [[CrossRef](#)]
38. Cennamo, N.; Massarotti, D.; Conte, L.; Zeni, L. Low Cost Sensors Based on SPR in a Plastic Optical Fiber for Biosensor Implementation. *Sensors* **2011**, *11*, 11752–11760. [[CrossRef](#)]
39. Cennamo, N.; D’Agostino, G.; Porto, G.; Biasiolo, A.; Perri, C.; Arcadio, F.; Zeni, L. A Molecularly Imprinted Polymer on a Plasmonic Plastic Optical Fiber to Detect Perfluorinated Compounds in Water. *Sensors* **2018**, *18*, 1836. [[CrossRef](#)]
40. Cennamo, N.; De Maria, L.; D’Agostino, G.; Zeni, L.; Pesavento, M. Monitoring of Low Levels of Furfural in Power Transformer Oil with a Sensor System Based on a POF-MIP Platform. *Sensors* **2015**, *15*, 8499–8511. [[CrossRef](#)] [[PubMed](#)]
41. Pesavento, M.; Zeni, L.; De Maria, L.; Alberti, G.; Cennamo, N. SPR-Optical Fiber-Molecularly Imprinted Polymer Sensor for the Detection of Furfural in Wine. *Biosensors* **2021**, *11*, 72. [[CrossRef](#)] [[PubMed](#)]
42. Cennamo, N.; Pesavento, M.; Marchetti, S.; Zeni, L. Molecularly Imprinted Polymers and Optical Fiber Sensors for Security Applications. In *Advanced Materials for Defense. Springer Proceedings in Materials*; Fangueiro, R., Rana, S., Eds.; Springer: Cham, Switzerland, 2020; Volume 4, pp. 17–24.
43. Cennamo, N.; D’Agostino, G.; Pesavento, M.; Zeni, L. High selectivity and sensitivity sensor based on MIP and SPR in tapered plastic optical fibers for the detection of L-nicotine. *Sens. Actuators B Chem.* **2014**, *191*, 529–536. [[CrossRef](#)]

44. Cennamo, N.; De Maria, L.; Chemelli, C.; Profumo, A.; Zeni, L.; Pesavento, M. Markers detection in transformer oil by plasmonic chemical sensor system based on POF and MIPs. *IEEE Sens. J.* **2016**, *16*, 7663–7670. [[CrossRef](#)]
45. Cennamo, N.; D'Agostino, G.; Perri, C.; Arcadio, F.; Chiaretti, G.; Parisio, E.M.; Camarlinghi, G.; Vettori, C.; Di Marzo, F.; Cennamo, R.; et al. Proof of Concept for a Quick and Highly Sensitive On-Site Detection of SARS-CoV-2 by Plasmonic Optical Fibers and Molecularly Imprinted Polymers. *Sensors* **2021**, *21*, 1681. [[PubMed](#)]
46. Dibekkaya, H.; Saylan, Y.; Yilmaz, F.; Derazshamshir, A.; Denizli, A. Surface plasmon resonance sensors for real-time detection of cyclic citrullinated peptide antibodies. *J. Macromol. Sci. Part A* **2016**, *53*, 585–594. [[CrossRef](#)]
47. Ayankojo, A.G.; Reut, J.; Öpik, A.; Furchner, A.; Syritski, V. Hybrid molecularly imprinted polymer for amoxicillin detection. *Biosens. Bioelectron.* **2018**, *118*, 102–107. [[CrossRef](#)] [[PubMed](#)]
48. Ertürk, G.; Mattiasson, B. From imprinting to microcontact imprinting—A new tool to increase selectivity in analytical devices. *J. Chromatogr.* **2016**, *1021*, 30–44. [[CrossRef](#)] [[PubMed](#)]
49. Perçin, I.; Idil, N.; Bakhshpour, M.; Yılmaz, E.; Mattiasson, B.; Denizli, A. Microcontact imprinted plasmonic nanosensors: Powerful tools in the detection of salmonella paratyphi. *Sensors* **2017**, *17*, 1375. [[CrossRef](#)] [[PubMed](#)]
50. Ertürk Bergdahl, G.; Andersson, T.; Allhorn, M.; Yngman, S.; Timm, R.; Lood, R. In vivo detection and absolute quantification of a secreted bacterial factor from skin using molecularly imprinted polymers in a surface plasmon resonance biosensor for improved diagnostic abilities. *ACS Sens.* **2019**, *4*, 717–725. [[CrossRef](#)] [[PubMed](#)]
51. Kidakova, A.; Reut, J.; Rappich, J.; Öpik, A.; Syritski, V. Preparation of a surface-grafted protein-selective polymer film by combined use of controlled/living radical photopolymerization and microcontact imprinting. *React. Funct. Polym.* **2018**, *125*, 47–56. [[CrossRef](#)]
52. Li, Y.; Li, X.; Dong, C.; Li, Y.; Jin, P.; Qi, J. Selective recognition and removal of chlorophenols from aqueous solution using molecularly imprinted polymer prepared by reversible addition-fragmentation chain transfer polymerization. *Biosens. Bioelectron.* **2009**, *25*, 306–312. [[CrossRef](#)] [[PubMed](#)]
53. Salian, V.D.; White, C.J.; Byrne, M.E. Molecularly imprinted polymers via living radical polymerization: Relating increased structural homogeneity to improved template binding parameters. *React. Funct. Polym.* **2014**, *78*, 38–46. [[CrossRef](#)]
54. Gonzato, C.; Courty, M.; Pasetto, P.; Haupt, K. Magnetic molecularly imprinted polymer nanocomposites via surface-initiated RAFT polymerization. *Adv. Funct. Mater.* **2011**, *21*, 3947–3953. [[CrossRef](#)]
55. Chou, P.C.; Rick, J.; Chou, T.C. C-reactive protein thin-film molecularly imprinted polymers formed using a micro-contact approach. *Anal. Chim. Acta* **2005**, *542*, 20–25. [[CrossRef](#)]
56. Ertürk, G.; Hedström, M.; Mattiasson, B. A sensitive and real-time assay of trypsin by using molecular imprinting-based capacitive biosensor. *Biosens. Bioelectron.* **2016**, *86*, 557–565. [[CrossRef](#)]
57. Osman, B.; Uzun, L.; Beşirli, N.; Denizli, A. Microcontact imprinted surface plasmon resonance sensor for myoglobin detection. *Mater. Sci. Eng. C* **2013**, *33*, 3609–3614. [[CrossRef](#)] [[PubMed](#)]
58. Malitesta, C.; Mazzotta, E.; Picca, R.A.; Poma, A.; Chianella, I.; Piletsky, S.A. MIP sensors—the electrochemical approach. *Anal. Bioanal. Chem.* **2012**, *402*, 1827–1846. [[CrossRef](#)] [[PubMed](#)]
59. Choi, S.W.; Chang, H.J.; Lee, N.; Kim, J.H.; Chun, H.S. Detection of mycoestrogen zearalenone by a molecularly imprinted polypyrrole-based surface plasmon resonance (SPR) sensor. *J. Agric. Food Chem.* **2009**, *57*, 1113–1118. [[CrossRef](#)]
60. Pernites, R.B.; Ponnampati, R.R.; Advincula, R.C. Surface plasmon resonance (SPR) detection of theophylline via electropolymerized molecularly imprinted polythiophenes. *Macromolecules* **2010**, *43*, 9724–9735. [[CrossRef](#)]
61. Pernites, R.B.; Ponnampati, R.R.; Felipe, M.J.; Advincula, R. Electropolymerization molecularly imprinted polymer (E-MIP) SPR sensing of drug molecules: Pre-polymerization complexed terthiophene and carbazole electroactive monomers. *Biosens. Bioelectron.* **2011**, *26*, 2766–2771. [[CrossRef](#)] [[PubMed](#)]
62. Hubilla, F.A.D.; Mabilangan, A.I.; Advincula, R.C.; del Mundo, F.R. A surface plasmon resonance histamine sensor based on an electropolymerized molecularly imprinted polymer (e-mip). *MATEC Web Conf.* **2017**, *95*, 02006. [[CrossRef](#)]
63. Gupta, G.; Singh, P.K.; Boopathi, M.; Kamboj, D.V.; Singh, B.; Vijayaraghavan, R. Molecularly imprinted polymer for the recognition of biological warfare agent staphylococcal enterotoxin B based on Surface Plasmon Resonance. *Thin Solid Film.* **2010**, *519*, 1115–1121. [[CrossRef](#)]
64. Gupta, G.; Bhaskar, A.S.; Tripathi, B.K.; Pandey, P.; Boopathi, M.; Rao, P.V.; Singh, B.; Vijayaraghavan, R. Supersensitive detection of T-2 toxin by the in situ synthesized π -conjugated molecularly imprinted nanopatterns. An in situ investigation by surface plasmon resonance combined with electrochemistry. *Biosens. Bioelectron.* **2011**, *26*, 2534–2540. [[CrossRef](#)] [[PubMed](#)]
65. Bartold, K.; Pietrzyk-Le, A.; Huynh, T.P.; Iskierko, Z.; Sosnowska, M.; Noworyta, K.; Lisowski, W.; Sannicolò, F.; Cauteruccio, S.; Licandro, E.; et al. Programmed transfer of sequence information into a molecularly imprinted polymer for hexakis (2, 2'-bithien-5-yl) DNA analogue formation toward single-nucleotide-polymorphism detection. *ACS Appl. Mater. Interfaces* **2017**, *9*, 3948–3958. [[CrossRef](#)] [[PubMed](#)]
66. Bartold, K.; Pietrzyk-Le, A.; Golebiewska, K.; Lisowski, W.; Cauteruccio, S.; Licandro, E.; D'Souza, F.; Kutner, W. Oligonucleotide determination via peptide nucleic acid macromolecular imprinting in an electropolymerized cg-rich artificial oligomer analogue. *ACS Appl. Mater. Interfaces* **2018**, *10*, 27562–27569. [[CrossRef](#)] [[PubMed](#)]
67. Sari, E.; Üzek, R.; Duman, M.; Denizli, A. Fabrication of surface plasmon resonance nanosensor for the selective determination of erythromycin via molecular imprinted nanoparticles. *Talanta* **2016**, *150*, 607–614. [[CrossRef](#)] [[PubMed](#)]
68. Yılmaz, E.; Özgür, E.; Bereli, N.; Türkmen, D.; Denizli, A. Plastic antibody based surface plasmon resonance nanosensors for selective atrazine detection. *Mater. Sci. Eng. C* **2017**, *73*, 603–610. [[CrossRef](#)]

69. Altintas, Z. Surface plasmon resonance based sensor for the detection of glycopeptide antibiotics in milk using rationally designed nanoMIPs. *Sci. Rep.* **2018**, *8*, 11222. [[CrossRef](#)] [[PubMed](#)]
70. Ashley, J.; Shukor, Y.; D'Aurelio, R.; Trinh, L.; Rodgers, T.L.; Temblay, J.; Pleasants, M.; Tothill, I.E. Synthesis of molecularly imprinted polymer nanoparticles for α -casein detection using surface plasmon resonance as a milk allergen sensor. *ACS Sens.* **2018**, *3*, 418–424. [[CrossRef](#)]
71. Erdem, Ö.; Saylan, Y.; Cihangir, N.; Denizli, A. Molecularly imprinted nanoparticles based plasmonic sensors for real-time enterococcus faecalis detection. *Biosens. Bioelectron.* **2019**, *126*, 608–614. [[CrossRef](#)]
72. Rahtuvanoğlu, A.; Akgönüllü, S.; Karacan, S.; Denizli, A. Biomimetic nanoparticles based surface plasmon resonance biosensors for histamine detection in foods. *ChemistrySelect* **2020**, *5*, 5683–5692. [[CrossRef](#)]
73. Cennamo, N.; Maniglio, D.; Tatti, R.; Zeni, L.; Bossi, A.M. Deformable molecularly imprinted nanogels permit sensitivity-gain in plasmonic sensing. *Biosens. Bioelectron.* **2020**, *156*, 112126. [[CrossRef](#)]
74. Cennamo, N.; Bossi, A.M.; Arcadio, F.; Maniglio, D.; Zeni, L. On the Effect of Soft Molecularly Imprinted Nanoparticles Receptors Combined to Nanoplasmonic Probes for Biomedical Applications. *Front. Bioeng. Biotechnol.* **2021**, *9*, 801489. [[CrossRef](#)]
75. Arcadio, F.; Seggio, M.; Del Prete, D.; Buonanno, G.; Mendes, J.; Coelho, L.C.C.; Jorge, P.A.S.; Zeni, L.; Bossi, A.M.; Cennamo, N. A Plasmonic Biosensor Based on Light-Diffusing Fibers Functionalized with Molecularly Imprinted Nanoparticles for Ultralow Sensing of Proteins. *Nanomaterials* **2022**, *12*, 1400. [[CrossRef](#)] [[PubMed](#)]
76. Üzek, R.; Özkara, S.; Güngüneş, H.; Uzun, L.; Şenel, S. Magnetic nanoparticles for plasmid DNA purification through hydrophobic interaction chromatography. *Sep. Sci. Technol.* **2014**, *49*, 2193–2203. [[CrossRef](#)]
77. Amin, M.M.; Zilles, J.L.; Greiner, J.; Charbonneau, S.; Raskin, L.; Morgenroth, E. Influence of the antibiotic erythromycin on anaerobic treatment of a pharmaceutical wastewater. *Environ. Sci. Technol.* **2006**, *40*, 3971–3977. [[CrossRef](#)] [[PubMed](#)]
78. Lian, W.; Liu, S.; Yu, J.; Xing, X.; Li, J.; Cui, M.; Huang, J. Electrochemical sensor based on gold nanoparticles fabricated molecularly imprinted polymer film at chitosan–platinum nanoparticles/graphene–gold nanoparticles double nanocomposites modified electrode for detection of erythromycin. *Biosens. Bioelectron.* **2012**, *38*, 163–169. [[CrossRef](#)]
79. Altintas, Z.; Gittens, M.; Guerreiro, A.; Thompson, K.A.; Walker, J.; Piletsky, S.; Tothill, I.E. Detection of waterborne viruses using high affinity molecularly imprinted polymers. *Anal. Chem.* **2015**, *87*, 6801–6807. [[CrossRef](#)]
80. Hoshino, Y.; Kodama, T.; Okahata, Y.; Shea, K.J. Peptide imprinted polymer nanoparticles: A plastic antibody. *J. Am. Chem. Soc.* **2008**, *130*, 15242–15243. [[CrossRef](#)] [[PubMed](#)]
81. Petryayeva, E.; Krull, U.J. Localized surface plasmon resonance: Nanostructures, bioassays and biosensing—A review. *Anal. Chim. Acta* **2011**, *706*, 8–24. [[CrossRef](#)]
82. Chauhan, M.; Singh, V.K. Review on recent experimental SPR/LSPR based fiber optic analyte sensors. *Opt. Fiber Technol.* **2021**, *64*, 102580. [[CrossRef](#)]
83. Ahmad, R.; Griffete, N.; Lamouri, A.; Felidj, N.; Chehimi, M.M.; Mangeney, C. Nanocomposites of gold nanoparticles@molecularly imprinted polymers: Chemistry, processing, and applications in sensors. *Chem. Mater.* **2015**, *27*, 5464–5478. [[CrossRef](#)]
84. Wu, L.; Li, X.; Miao, H.; Xu, J.; Pan, G. State of the art in development of molecularly imprinted biosensors. *View* **2022**, *3*, 20200170. [[CrossRef](#)]
85. Abbas, A.; Tian, L.; Morrissey, J.J.; Kharasch, E.D.; Singamaneni, S. Hot spot-localized artificial antibodies for label-free plasmonic biosensing. *Adv. Funct. Mater.* **2013**, *23*, 1789–1797. [[CrossRef](#)]
86. Hu, R.; Luan, J.; Kharasch, E.D.; Singamaneni, S.; Morrissey, J.J. Aromatic functionality of target proteins influences monomer selection for creating artificial antibodies on plasmonic biosensors. *ACS Appl. Mater. Interfaces* **2017**, *9*, 145–151. [[CrossRef](#)]
87. Guerreiro, J.R.L.; Teixeira, N.; De Freitas, V.; Sales, M.G.F.; Sutherland, D.S. A saliva molecular imprinted localized surface plasmon resonance biosensor for wine astringency estimation. *Food Chem.* **2017**, *233*, 457–466. [[CrossRef](#)]
88. Culver, H.R.; Wechsler, M.E.; Peppas, N.A. Label-free detection of tear biomarkers using hydrogel-coated gold nanoshells in a localized surface plasmon resonance-based biosensor. *ACS Nano* **2018**, *12*, 9342–9354. [[CrossRef](#)]
89. Chen, B.; Liu, C.; Sun, X.; Hayashi, K. Molecularly imprinted polymer coated Au nanoparticle sensor for α -pinene vapor detection. In Proceedings of the SENSORS, 2013 IEEE, Baltimore, MD, USA, 4–6 November 2013.
90. Shang, L.; Liu, C.; Chen, B.; Hayashi, K. Development of molecular imprinted sol-gel based LSPR sensor for detection of volatile cis-jasmone in plant. *Sens. Actuators B Chem.* **2018**, *260*, 617–626. [[CrossRef](#)]
91. Bagherpour, M.B.; Nikazar, M.; Welander, U.; Bonakdarpour, B.; Sanati, M. Effects of irrigation and water content of packings on alpha-pinene vapours biofiltration performance. *Biochem. Eng. J.* **2005**, *24*, 185–193. [[CrossRef](#)]
92. Misra, G.; Pavlostathis, S.G.; Perdue, E.M.; Araujo, R. Aerobic biodegradation of selected monoterpenes. *Appl. Microbiol. Biotechnol.* **1996**, *45*, 831–838. [[CrossRef](#)]
93. Mohseni, M.; Allen, D.G. Biofiltration of mixtures of hydrophilic and hydrophobic volatile organic compounds. *Chem. Eng. Sci.* **2000**, *55*, 1545–1558. [[CrossRef](#)]
94. Dhamwichukorn, S.; Kleinheinz, G.T.; Bagley, S.T. Thermophilic biofiltration of methanol and α -pinene. *J. Ind. Microbiol. Biotechnol.* **2001**, *26*, 127–133. [[CrossRef](#)] [[PubMed](#)]
95. Chegel, V.I.; Lopatynskyi, A.M.; Lytvyn, V.K.; Demydov, P.V.; Martínez-Pastor, J.P.; Abargues, R.; Gadea, E.A.; Piletsky, S.A. Localized surface plasmon resonance nanochips with molecularly imprinted polymer coating for explosives sensing. *Semicond. Phys. Quantum Electron.* **2020**, *23*, 431–436. [[CrossRef](#)]

96. Wang, W.; Wang, R.; Liao, M.; Kidd, M.T.; Li, Y. Rapid detection of enrofloxacin using a localized surface plasmon resonance sensor based on polydopamine molecular imprinted recognition polymer. *J. Food Meas. Charact.* **2021**, *15*, 3376–3386. [[CrossRef](#)]
97. Underner, M.; Grignon, B.; Roblot, F.; Meurice, J.C.; Patte, F. Fluoroquinolones: Pharmacology, antibacterial spectrum and indications in pneumology. *Rev. Pneumol. Clin.* **1989**, *45*, 14–22. [[PubMed](#)]
98. Nemeth, J.; Oesch, G.; Kuster, S.P. Bacteriostatic versus bactericidal antibiotics for patients with serious bacterial infections: Systematic review and meta-analysis. *J. Antimicrob. Chemother.* **2015**, *70*, 382–395. [[CrossRef](#)] [[PubMed](#)]
99. Hooper, D.C. Mechanisms of action of antimicrobials: Focus on fluoroquinolones. *Clin. Infect. Dis.* **2001**, *32*, S9–S15. [[CrossRef](#)] [[PubMed](#)]
100. Holland, W.R.; Hall, D.G. Surface-plasmon dispersion relation: Shifts induced by the interaction with localized plasma resonances. *Phys. Rev. B* **1983**, *27*, 7765–7768. [[CrossRef](#)]
101. Frasconi, M.; Tel-Vered, R.; Riskin, M.; Willner, I. Surface plasmon resonance analysis of antibiotics using imprinted boronic acid-functionalized Au nanoparticle composites. *Anal. Chem.* **2010**, *82*, 2512–2519. [[CrossRef](#)]
102. Riskin, M.; Tel-Vered, R.; Frasconi, M.; Yavo, N.; Willner, I. Stereoselective and chiroselective surface plasmon resonance (SPR) analysis of amino acids by molecularly imprinted Au-nanoparticle composites. *Chem. Eur. J.* **2010**, *16*, 7114–7120. [[CrossRef](#)]
103. Ben-Amram, Y.; Riskin, M.; Willner, I. Selective and enantioselective analysis of mono- and disaccharides using surface plasmon resonance spectroscopy and imprinted boronic acid-functionalized Au nanoparticle composites. *Analyst* **2010**, *135*, 2952–2959. [[CrossRef](#)]
104. Akgönüllü, S.; Yavuz, H.; Denizli, A. SPR nanosensor based on molecularly imprinted polymer film with gold nanoparticles for sensitive detection of aflatoxin B1. *Talanta* **2020**, *219*, 121219. [[CrossRef](#)]
105. Akgönüllü, S.; Yavuz, H.; Denizli, A. Development of Gold Nanoparticles Decorated Molecularly Imprinted-Based Plasmonic Sensor for the Detection of Aflatoxin M1 in Milk Samples. *Chemosensors* **2021**, *9*, 363. [[CrossRef](#)]
106. Türkmen, D.; Bakhshpour, M.; Göktürk, I.; Aşır, S.; Yılmaz, F.; Denizli, A. Selective dopamine detection by SPR sensor signal amplification using gold nanoparticles. *New J. Chem.* **2021**, *45*, 18296–18306. [[CrossRef](#)]
107. Lee, K.H.; Su, Y.D.; Chen, S.J.; Lee, G.B. 2-Dimensional SPR Detection System Integrated with Molecular Imprinting Polymer Microarrays Using Microfluidic Technology. In Proceedings of the 19th IEEE International Conference on Micro Electro Mechanical Systems, Istanbul, Turkey, 22–26 January 2006; pp. 430–433.
108. Lautner, G.; Kaev, J.; Reut, J.; Öpik, A.; Rappich, J.; Syritski, V.; Gyurcsányi, R.E. Selective artificial receptors based on micropatterned surface-imprinted polymers for label-free detection of proteins by SPR Imaging. *Adv. Funct. Mater.* **2011**, *21*, 591–597. [[CrossRef](#)]
109. Bossert, M.; Erdőssy, J.; Lautner, G.; Witt, J.; Köhler, K.; Gajovic-Eichelmann, N.; Yarman, A.; Wittstock, G.; Scheller, F.W.; Gyurcsányi, R.E. Microelectrospotting as a new method for electrosynthesis of surface-imprinted polymer microarrays for protein recognition. *Biosens. Bioelectron.* **2015**, *73*, 123–129. [[CrossRef](#)] [[PubMed](#)]
110. Luo, Q.; Yu, N.; Shi, C.; Wang, X.; Wu, J. Surface plasmon resonance sensor for antibiotics detection based on photo-initiated polymerization molecularly imprinted array. *Talanta* **2016**, *161*, 797–803. [[CrossRef](#)] [[PubMed](#)]

Disclaimer/Publisher’s Note: The statements, opinions and data contained in all publications are solely those of the individual author(s) and contributor(s) and not of MDPI and/or the editor(s). MDPI and/or the editor(s) disclaim responsibility for any injury to people or property resulting from any ideas, methods, instructions or products referred to in the content.